論文 / 著書情報
Article / Book Information

題目(和文)	ヒト多能性幹細胞から膵臓β細胞への分化誘導における亜鉛役割の解明
Title(English)	Elucidating the role of zinc in pancreatic β cell differentiation using human pluripotent stem cells
著者(和文)	ｴﾘｰﾝｼﾝ ﾂｰｼｪﾝ
Author(English)	Zixuan Erinn Sim
出典(和文)	学位:博士(学術), 学位授与機関:東京工業大学, 報告番号:甲第12249号, 授与年月日:2022年9月22日, 学位の種別:課程博士, 審査員:粂 昭苑,白木 伸明,木村 宏,山口 雄輝,小倉 俊一郎
Citation(English)	Degree:Doctor (Academic), Conferring organization: Tokyo Institute of Technology, Report number:甲第12249号, Conferred date:2022/9/22, Degree Type:Course doctor, Examiner:,,,,
学位種別(和文)	博士論文
Type(English)	Doctoral Thesis

Doctoral Degree Dissertation

Elucidating the role of zinc in pancreatic β cell differentiation using human pluripotent stem cells

Erinn Sim Zixuan

Life Science and Technology

School of Life science and Technology

Tokyo Institute of Technology

Table of Contents

Presentation Abstract

Background

Human pluripotent stem cells (hPSCs) have a high proliferation rate and the ability to differentiate into all major somatic cell lineages, potentially for use in cell replacement therapy, drug discovery, and disease modeling. Here, we focus on the importance of nutrient components in culture media to generate hPSC-derived pancreatic β cells to provide an alternative cell source for islet transplantation. We found that undifferentiated hPSCs are in an active state of methionine catabolism from the past results of gene expression and metabolites analysis. Five hours of methionine deprivation (ΔMet) in culture media of hPSCs resulted in a rapid decrease in intracellular S-adenosyl methionine, SAM. The decrease in SAM content placed the cells at a biased state for differentiation specifically in comparison to complete (Compl) and other amino acid deprivation pretreated hPSCs (Shiraki et al., 2014). From the microarrays results using Compl and ΔMet pretreated cells, 18 common upregulated genes with significant differences, including *SLC30A1*, were observed in ΔMet cells. *SLC30A1* encodes a zinc exporter found on the plasma membrane, ZNT1. Therefore, upregulation of ZNT1 theoretically results in decreasing intracellular Zinc (Zn) concentration. From these results, I hypothesized that the elevated differentiation potency after ΔMet treatment of hPSCs might be due to the changes of Zn contents in the cells. Therefore, my research aim is to understand Zn's roles in the maintenance culture of undifferentiated hPSCs and pancreatic differentiation, lastly, to reveal the interaction between Zn and Met.

Results

• Zinc (Zn) is necessary for cell survival of undifferentiated hPSCs

I introduced a Zn-deprived (ΔZn) custom-made media to investigate the effect of Zn on hPSCs. Insulin growth factor 1 (IGF1) is used to substitute insulin (INS) supplements as INS contains excess Zn ions for structural stability. Undifferentiated hPSCs were cultured with maintenance media supplemented with IGF1 and graded Zn for 3 days. The cells were then sampled and analyzed for cell proliferation (EdU incorporation) and gene expression (real-time PCR). Cells cultured under 0 μM Zn exhibited lower DAPI+ cells count and decreased EdU+ cell population, indicating reduced proliferation rate compared to control, 3 μM Zn. Furthermore, hPSCs cultured under 0, 0.5, 1 μM Zn showed significant downregulation of cell renewal markers, *GRB7*, and *HCK* and upregulation of differentiation markers, *GATA4*, *PECAM* and *PAX6* compared to controls, suggesting an increased differentiation potency towards all three germ layers.

• Zn addition reduced endoderm differentiation efficiency and impacted pancreatic differentiation

Knowing that ΔZn triggers differentiation, I then investigate the effect of Zn in definitive endoderm (DE) and pancreatic differentiation. First, hPSCs were pretreated with 5h of Compl and ΔMet, and then DE differentiation was initiated under Zn added conditions (0, 0.5, 3 μM).

As a result, cells expressing the pluripotency marker, OCT3/4, increased proportionately to the increase in Zn. Also, the addition of 3 μM Zn in Compl pretreated cells led to a reduced proportion of SOX17+ cells. While in ΔMet, DE differentiation was efficient in all three Zn concentrations. This result suggested that Zn addition reduced DE differentiation efficiency, and ΔMet pretreatment overrides the effects of Zn. Next, IGF1-supplemented differentiation media with Zn added conditions were used to differentiate pancreatic progenitor and endocrine cells. The cell numbers decreased drastically under all Zn concentrations. Considering instead of IGF1, INS might be needed for cell survival. I then change the supplement to insulin glulisine (Zn-absence mutated INS), and cells managed to survive till the end of differentiation. Also, cells cultured under 3 μM Zn showed a higher percentage in pancreatic marker, NKX6.1+ cells among PDX1+ cell population compared to 0 μM Zn, suggesting that Zn and INS contribute to endocrine progenitor differentiation efficiency.

• The link between Zn signaling and Met metabolism in undifferentiated hPSCs

RNA sequencing was performed to analyze the global expression profile of hPSCs cultured under graded Zn concentration. The results were compared with ΔMet cells. Zn and ΔMet responsive genes include *EGR1*, *MT1H*, *PIM1, SLC30A1*, and *TNFRSF12A*. The common genes downregulated in Zn added and ΔMet cells contain *FLT1*, *GDF3*, *P2RY1*, *SLC39A6*, *TET1*, and *USP12*. ΔZn cultured cells exhibited changes in gene expressions related to the Met cycle, such as *MAT2A* and *DNMT3B*. The relationship between Met and Zn was confirmed by analyzing intracellular Met-cycle metabolites in cells cultured at different Zn concentrations. A decrease in intracellular SAM level was observed in ΔZn cells, similar results were seen in ΔMet cells, revealing the link between Met metabolism and Zn signaling.

Conclusion

Overall, I focused on Zn in culture media and found that Zn supports hPSCs cell growth. Zn addition reduced DE differentiation and impacted pancreatic differentiation. Although Zn and Met share similar effects in regulating the maintenance and differentiation of hPSCs, the exact molecular mechanism linking Zn and Met is yet to be confirmed. In short, my novel differentiation procedure was applicable in generating functional pancreatic β cells and may be used for further application in regenerative medicine.

Acknowledgments

First, I would like to thank my doctoral degree advisors, Professor Shoen Kume and Associate Professor Nobuaki Shiraki of the School of Life Science and Technology at Tokyo Institute of Technology. Professor Kume consistently allowed this whole research and thesis to be my work but steered me in the right direction whenever she thought I needed it. Associate Professor Shiraki is always there for discussions whenever I ran into a trouble spot or had a question about my experiments and dissertation writing. At the final stage of my degree, they spared their precious time for various discussion sessions for my publication, presentation practice, and dissertation writing.

Furthermore, I would like to thank Ajinomoto Co., Inc. for providing the zinc/insulin-deprived basal media which is still not commercially available. I would also like to thank Center for iPS Cell Research and Application (CiRA), Kyoto University for the human induced pluripotent stem cell stock supply. Also, thank you Miura Laboratory, especially Dr. Soshiro Kashio from Tokyo University for performing the measurements of metabolites (Figure 5.3DE). I am grateful for the help of Associate Professor Taiho Kambe from Kyoto University in providing the anti-ZNT1 antibody. The following invaluable contributions also cannot be underestimated. Experiments in Figure 2.3B-F were done in cooperation with Nao Furuta (previous member of Kume & Shiraki laboratory) and Akihiro Arakawa (Ajinomoto Co., Inc.). Experiments in Figure 4.3B-E were done with the help of Dr. Takayuki Enomoto (previous member of Kume & Shiraki laboratory). RNA sequencing analyses were done with cooperation of Hiroki Ozawa and Associtate Professor Shiraki. Without their participation, this research could not have been successfully conducted.

Finally, I must express my very profound gratitude to my parents, friends, and members of Kume & Shiraki laboratory for providing me with unfailing support and continuous encouragement throughout the process of researching and writing this dissertation. This accomplishment would not have been possible without them.

Thank you.

List of Abbreviations

ΔMet/AA	Methionine/amino acid deprivation
CDH5	Cadherin-5 precursor
COL1A1	Collagen Type I Alpha 1
DAPI	4',6-diamidino-2-phenylindole
DE	Definitive Endoderm
DNMT3B	DNA Methyltransferase 3 Beta
EC	Endocrine cells
EOMES	Eomesodermin
GAPDH	Glyceraldehyde 3-phosphate dehydrogenase
GRB7	Growth factor receptor-bound protein 7
HCK	Hemopoietic cell kinase
IGF1	Insulin-like Growth Factor 1
INS	Insulin
ISL1	Insulin Gene Enhancer Protein ISL1
NKX6.1	NK6 homeobox Protein
POU5F1	POU domain, class 5 transcription factor 1; also known as OCT3/4
PAX6	Paired box 6
PBS	Phosphate Buffered Saline
PECAM	Platelet Endothelial Cell Adhesion Molecule
PDX1	Pancreatic and Duodenal Homeobox 1
PP	Pancreatic Progenitor
PSCs	Pluripotent Stem Cells
SLC30A1	Solute Carrier Family 30 Member 1
SOX17	SRY- related HMG-box 17
TERT	Telomerase reverse transcriptase
ZFP42	Zinc finger protein 42
ZIP	Protein encoded by Solute Carrier Family 39 (zinc influx transporter)
Zn	Zinc
ZNT	Protein encoded by Solute Carrier Family 30 (zinc efflux transporter)

Chapter 1: Literature Review

1.1 Zinc and its importance to human health

Zinc (Zn) is the second most abundant essential trace metal next to iron for the development and growth of humans and animals. Zn is mainly localized in skeletal muscle and bone. In general, there are only 2-3 grams of Zn in 40-70 kilograms of an adult human body weight. However, Zn is known to be important for biological functions which can be grouped into three general groups: structural (zinc finger), catalytic (act as enzyme cofactors), and signaling mediating functions (in regulating Zn absorption, distribution, cellular uptake, and excretion) (Chasapis et al., 2012; Kambe et al., 2015; Yanagisawa and Nodera, 2007; Zoroddu et al., 2019).

As Zn is an essential element in supporting biological functions and can only obtain from the diet, daily intake of Zn is necessary. Lack of Zn intake can cause major sicknesses such as growth retardation, cell-mediated immune dysfunction, and cognitive impairment. On the other hand, excess Zn intake will cause abdominal pain, nausea, vomiting, and diarrhea, resulting in Zn poisoning (Fukada and Kambe, 2011; Roohani et al., 2013; Yanagisawa and Nodera, 2007).

1.2 Zinc transporter proteins

Zn homeostasis is regulated through zinc transporters and metallothionein (MT). There are two Zn transporter protein families being identified in humans and animals, which function to regulate Zn homeostasis (Huang and Tepaamorndech, 2013; Jeong and Eide, 2013; Baltaci and Yuce, 2018). They are ZNT (encoded by SLC30A gene) and ZIP (encoded by SLC39A gene). There are 10 ZNT and 14 ZIP transporters found in the human genome localized in cells (Figure 1A). ZNT is responsible for the Zn efflux that transfers Zn out of the cytoplasm while ZIP is for the Zn influx (Figure 1B).

Metallothionein (MT) is known to bind seven Zn atoms, which likely takes part in the uptake, transport, and regulation of Zn in the human body. By the binding and releasing of Zn ions, MT involves in the roles of cell growth and differentiation and appears to influence the growth or survival of tumor cells. They also function as antioxidants, protecting cells against hydroxyl free radicals (Maret, 2000; Takahashi, 2012; Thirumoorthy et al., 2007; Wang et al., 2014).

Figure 1A

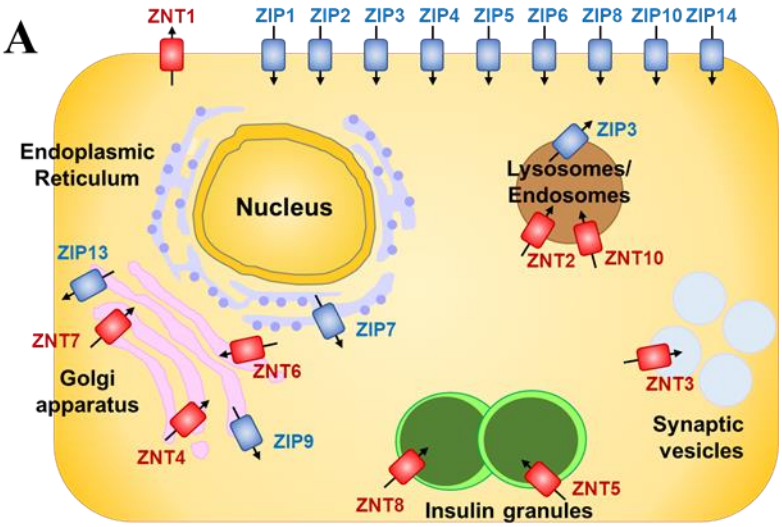

B

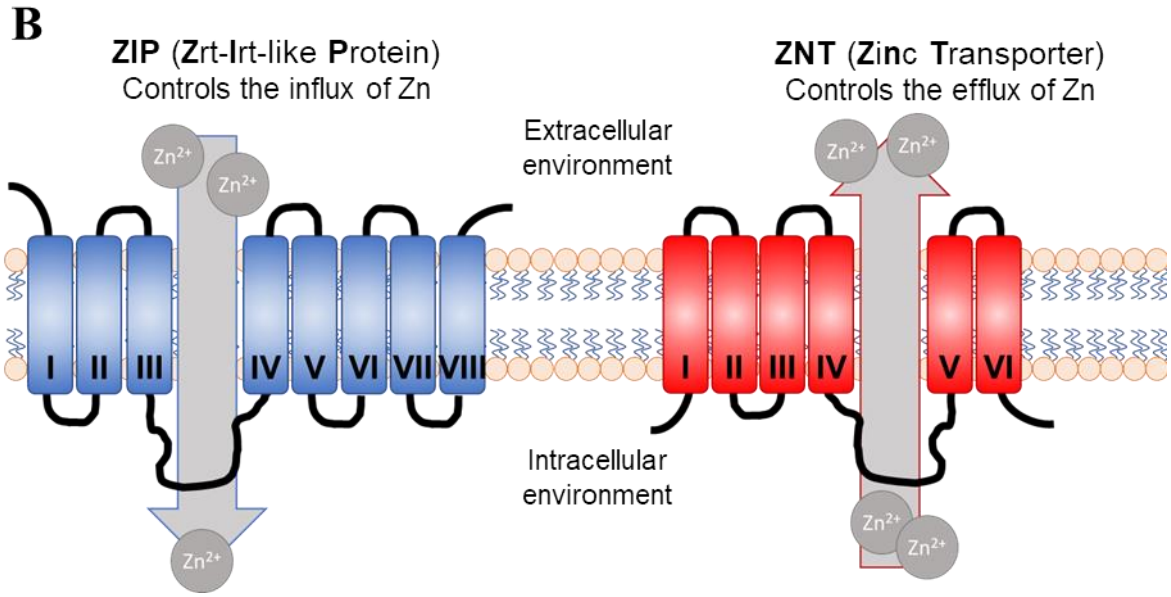

Figure 1

A: Illustration showing localization and direction of Zn mobilization by ZNT (red arrows) and ZIP (blue arrows).

(Adopted from Jeong and Eide, 2013; Kambe et al., 2015; Baltaci and Yuce, 2018 with modifications)

B: Putative structures together with the transport mechanisms of ZNT and ZIP transporters. ZNT controls the efflux of Zn while ZIP controls the influx of extracellular or vesicular in the opposite direction.

(Adopted from Kambe et al., 2015 with modifications)

1.3 Pancreatic β cell differentiation using human pluripotent stem cells

Human pluripotent stem cells (PSCs) include embryonic stem cells (ESCs) and induced pluripotent stem cells (iPSCs). ESCs are derived from the inner cell mass of a blastocyst. They possess the ability to proliferate unlimitedly and to differentiate into any cell type (Thomson et al., 1998). Next are iPSCs, they work just like ESCs. They were created by Prof. Yamanaka's group, through the introduction of four specific genes: *OCT3/4* (or *POU5F1*), *SOX2*, *KLF4*, *c-MYC* into adult somatic cells (Takahashi and Yamanaka, 2006). Similar to ESCs, iPSCs have a high proliferation rate and the potential to differentiate into major somatic cell types. Therefore, PSCs have a great capacity for cell replacement therapy, drug discovery, and disease modeling (Inoue et al., 2014; Sánchez Alvarado and Yamanaka, 2014; Takahashi and Yamanaka, 2016).

In Kume & Shiraki laboratory, we are working on the generation of pancreatic β cells derived from PSCs. The goal is to provide an alternative cell source for pancreas or islet transplantation. As pancreas or islet transplantation is a way to cure severe diabetes mellitus patients, the lack of donors remains a problem. Generating functional pancreatic β cells or islet cells using PSCs is a possible and promising solution for donor shortage. As progress had been made in this research field, directed differentiation of functional pancreatic β cells from PSCs has become feasible (Kroon et al., 2008; Millman et al., 2016; Pagliuca et al., 2014; Rezania et al., 2014; Velazco-Cruz et al., 2019; Zhang et al., 2009). In our lab, we also managed to establish a xeno-free culture system for insulin-producing β cells from PSCs (Shahjalal et al., 2014).

All the directed differentiation protocols were established by mimicking the *in vivo* pancreatic developmental process. Stepwise pancreatic differentiation procedure was performed in differentiating PSCs into definitive endoderm (DE), primitive gut tube (PG), pancreatic progenitor (PP), endocrine progenitor (EP), then into hormone-expressing endocrine cells (EC). Combined treatment of growth factors and small molecules were used in inhibiting or activating various signaling pathways which led to the generation of functional pancreatic β cells (Figure 1C) (Sim et al., 2021). Genes specifically expressed at each stage were used to evaluate the cells' differentiation efficiency. In the past decades, researchers had been focusing on growth factors and small molecules in culture media to generate a high yield of functional pancreatic β cells. Now, this can be achieved following the published protocols. Recent studies focus more on the cell culture microenvironment in generating differentiated cells and the molecular characteristics of PSC-derived pancreatic β cells.

Figure 1C

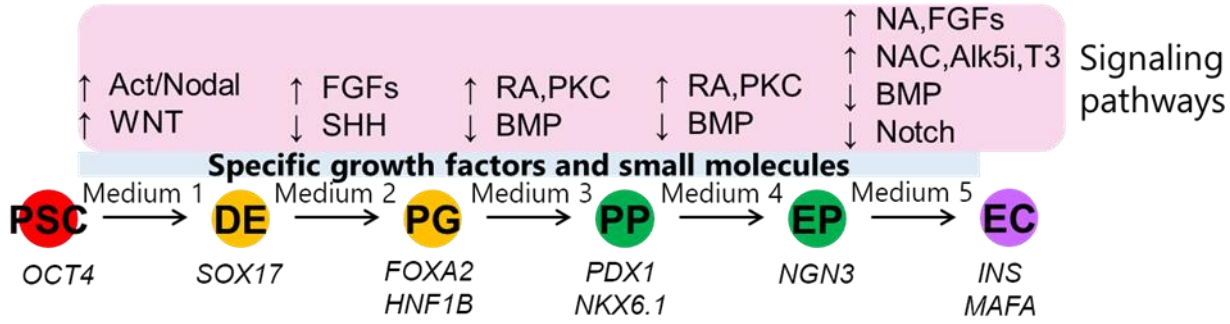

Figure 1

C: A schematic diagram of the differentiation procedure. PSCs are differentiated through five stages; each stage utilized the activation (↑) or inhibition (↓) of stated signaling pathways. Genes specifically expressed at each stage are shown at the lower part.

PSC: pluripotent stem cell, DE: definitive endoderm, PG: primitive gut tube, PP: pancreatic progenitor, EP: endocrine progenitor. EC: endocrine cell, SHH: sonic hedgehog, FGF: fibroblast growth factor, BMP: bone morphogenic protein, RA: retinoic acid, PKC: protein kinase C, NA: nicotinamide, NAC: N-acetylcysteine, Alk5i: transforming growth factor-beta receptor inhibitor, T3: thyroid hormone

1.4 Roles of Zinc found in pluripotent stem cells and pancreatic islet cells

As Zn is actively involved in regulating cellular signaling pathways, its role in pluripotent stem cells (PSCs) had been investigated. It is being reported that in mouse ESCs, 2 μM of zinc chloride ($ZnCl_2$) transiently maintained mouse ESCs pluripotency in vitro. The addition of Zn (2 μM $ZnCl_2$) in cell culture leads to upregulation of undifferentiation marker genes, *Oct4*, *Sox2*, *Nanog*, and downregulation marker genes, *Sox1*, *T*, *Gata4* (Hu et al., 2016). Another report also demonstrated that the number of mouse ESCs colonies increased monotonically as the extracellular concentration of Zn does (Mnatsakanyan et al., 2019). These results suggesting that Zn has an important role in maintaining cell pluripotency of mouse ESCs.

Furthermore, Zn was reported to promote neuronal differentiation in human PSCs. The number of iPSC-derived neural stem cell clusters was significantly reduced in zinc-deficient conditions, indicating a reduction in cell survival (Pfaender et al., 2016). In neural differentiation of iPSCs, the expression level of Nestin (neural stem cell marker) was higher in the $ZnCl_2$ (2.5, 5, and 10 μM) added group compared to the control (Yang et al., 2020). Ectoderm and mesoderm markers (*Brachyury/T* and *Sox1*) were upregulated in mouse ESCs treated with 100 μM of Zn under accelerated differentiation conditions (Mnatsakanyan et al., 2019). Other than that, endodermal and mesodermal differentiation using PSCs with consideration of Zn concentrations in culture media was not clearly being studied.

On the other hand, Zn appears to be a vital component for insulin-secreting cells (Chimienti et al., 2005). ZNT8 is a zinc transporter protein, which is highly expressed on the membrane of pancreatic beta cells. Total Zn content was reduced in ZnT8-deficient mouse islets and glucose-stimulated insulin secretion from isolated islets was reduced compared to wild-type (Pound et al., 2009). It is also reported that insulin-dense core granules were observed in wild-type mice but not in ZnT8-deficient mice, as ZnT8 is responsible for delivery of Zn into these insulin-containing granules for insulin maturation and storage (Lemaire et al., 2012). On the other hand, low expression of ZnT8 in mice resulted in decreasing insulin output from the β cell, while reduced Zn ions production favors clearance of the hormone by the liver (Rutter and Chimienti, 2015). Thus emphasized the importance of Zn in pancreatic β cells, that ZnT8 is required for the accumulation of zinc for proper insulin processing. However, this was only shown in mature β cells. The roles of zinc in generating pancreatic beta cells using human iPS cells were unknown.

1.5 Unique amino acid metabolism in pluripotent stem cells

There are 20 different types of amino acids that exist in our human body. They are divided into three different groups: essential (Threonine, Valine, Isoleucine, Leucine, Lysine, Histidine, Phenylalanine, Tryptophan, Methionine), conditionally essential (Arginine, Cysteine, Glutamine, Glycine, Proline, Tyrosine), and nonessential (Alanine, Asparagine, Aspartic acid, Glutamic acid, Serine) amino acids. These amino acids make up the proteins in the human body and play an important role in body functions.

Among growth factors that were being used for cell culture systems, amino acids are well-studied for PSCs culture settings (Liu et al., 2019). The amino acids in the cell culture are key components to maintain cell pluripotency. In this chapter, I will introduce a few research about the study of amino acids in the maintenance of pluripotency and in the differentiation induction of PSCs.

1.5.1 Presence of Proline in cell culture regulates mouse ESCs differentiation

Proline is mostly found in collagen, which is made up of the protein of skin, tendons, bones, and connective tissue. Also, proline was found with significantly higher concentrations in umbilical venous plasma (Cetin et al., 2005) and was reported to an important role in fetal survival, growth, and development (Wu et al., 2008). Addition of more than 100 μM proline into mouse ESCs cell culture-induced differentiation to a primitive ectoderm-like cell, through activation of the mTOR pathway (Washington et al., 2010). Another group proposed that proline induce mouse ESC transformation into mesenchymal stem cells, accompanied by a significant increase in histone H3 lysine-9 (H3K9) and histone H3 lysine-36 (H3K36) methylation levels (Comes et al., 2013).

1.5.2 Threonine involves in regulating the maintenance of mouse ESCs

Threonine is an essential amino acid that cannot be produced in the human body. It must be consumed through diet and is needed to create glycine and serine. Threonine dehydrogenase (TDH) converts threonine to glycine (for single carbon metabolism) and to acetyl-CoA (use in TCA cycle for energy production), which contributes to mouse ESCs cell survival (Chen and Wang, 2014). Cell proliferation of mouse ESCs is regulated by threonine via phosphorylation of Akt, ERK, p38, JNK/SAPK, and

mTOR signaling pathways (Ryu and Han, 2011). On the other hand, culturing mouse ESCs under threonine-deprived conditions decreased accumulation of S-adenosyl-methionine (SAM) and decreased trimethylation of histone H3 lysine-4 (H3K4me3), elevating cell differentiation (Shyh-Chang et al., 2013).

1.5.3 Methionine metabolism regulates the maintenance and differentiation of hPSCs

Methionine is another essential amino acid that needs to be obtained from the diet. Undifferentiated human PSCs are shown to be in a high-methionine metabolic state that decreased with differentiation (Shiraki et al., 2014). Undifferentiated PSCs were cultured under single deprivation of nine essential amino acids (threonine, valine, isoleucine, leucine, lysine, histidine, phenylalanine, tryptophan, methionine) condition for two days. Decreased total cell number was observed under leucine, lysine, tryptophan, and methionine-deprived cells. Most impacts were observed in methionine deprivation, as the cell number decreased lower than 5%. Similar to threonine deprivation of mouse ESCs, methionine deprivation led to a rapid decrease in SAM levels in the methionine metabolic cycle (Figure 1D). The reduction of SAM triggers p53 signaling, reduces the expression of pluripotency marker NANOG, and promotes cell differentiation into three germ layers (Figure 1E). Other groups also reported the application of methionine deprivation in removing undifferentiated PSCs and promoting cell differentiation. Human iPSC-derived cardiac cell sheets were treated with a methionine-free condition, in an attempt to remove iPS cell contamination (Matsuura et al., 2015). Also in cell differentiation culture of murine small intestinal organoids, the group proved that 24 hours of methionine deprivation markedly suppressed cell proliferation, thereby promoted differentiation (Saito et al., 2017). In this dissertation, I will also discuss some results on methionine deprivation in pancreatic differentiation and its link with Zn.

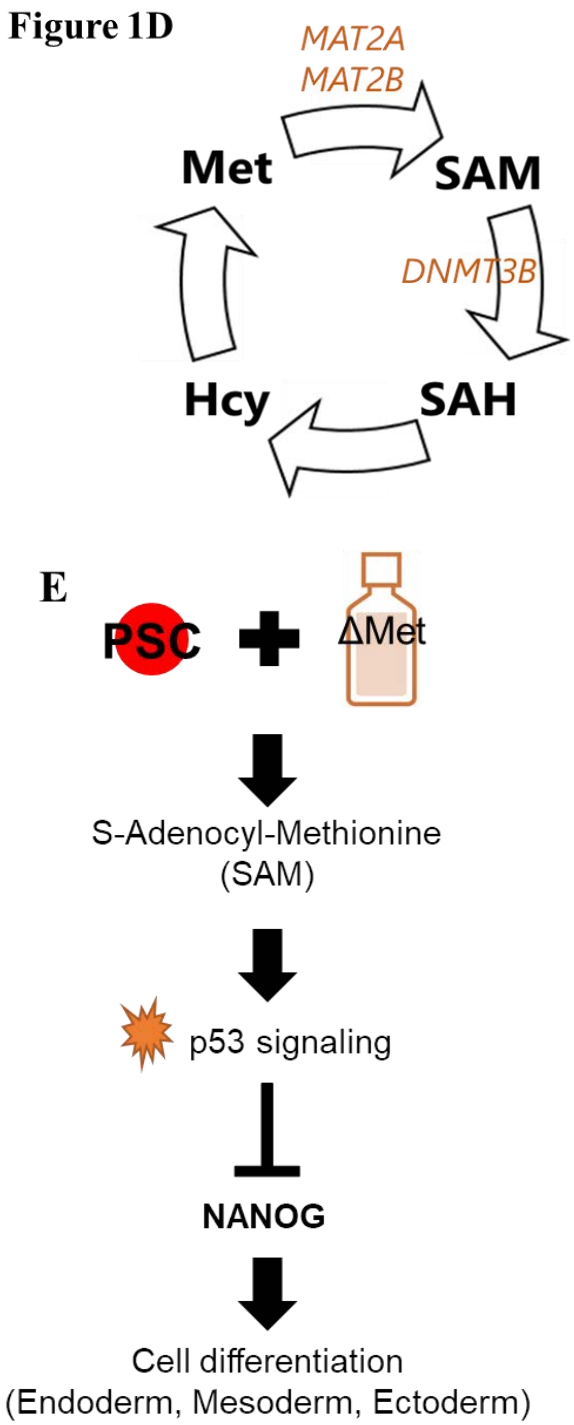

Figure 1

D: A schematic diagram showing the methionine cycle. Met: Methionine, SAM: S-adenosyl methionine, SAH: S-adenosyl homocysteine, HCY: Homocysteine

E: Schematic diagram showing undifferentiated PSCs being treated with methionine deprived (ΔMet) medium, resulting in decreased S-adenosyl-methionine (SAM) levels, triggered p53 signaling, decreased NANOG expression, and potentiated cell differentiation into three germ layers.

1.6 Aim and objectives

In Kume & Shiraki lab, we focus on the importance of nutrients components in the culture media to seek a favorable procedure to generate functional pancreatic β cells derived from human pluripotent stem cells (PSCs). Among the cell culture components, an essential amino acid, Methionine (Met) was found to be an important component in regulating the maintenance and differentiation of PSCs. However, the mechanism of Met involving cell differentiation remains unknown. Therefore, I aimed to seek the key factor that leads to differentiation potency after Met deprivation.

Continuing from our past research (Shiraki et al., 2014), I performed pancreatic differentiation using Met deprivation pretreated PSCs. This brought my attention to a Zn exporter, SLC30A1, which was specifically upregulated under Met deprivation compared to control (Chapter 2). Then, I attempted to investigate the effect of Zn in undifferentiated PSCs (Chapter 3) and in pancreatic differentiation (Chapter 4). Lastly, I also tried to determine the relationship between Met and Zn to reveal their connection in contributing to the maintenance culture of PSCs (Chapter 5).

1.7 Chapter Overview

Chapter 2: Methionine metabolism regulates maintenance of pluripotent stem cells and differentiation into pancreatic β cells

From the past results of gene expression and metabolites analysis, it is shown that undifferentiated PSCs are in an active state of methionine catabolism (Shiraki et al., 2014). As short as five hours of methionine deprivation (ΔMet) pretreatment in culture media of undifferentiated PSCs resulted in a rapid decrease in intracellular-S-adenosyl methionine (SAM). The reduction of SAM triggers p53 signaling, reduces the expression of pluripotency marker NANOG, and promotes cell differentiation into three germ layers. As follow up studies of the paper, I explored whether if ΔMet pretreatment could potentiate endoderm and the late-stage differentiation into pancreatic β cells. Therefore, in chapter 2, I will present the results of *in vitro* pancreatic differentiation using ΔMet pretreated PSCs. Also, I will discuss how Zn become the focus of my research.

Chapter 3: Roles of Zinc in maintenance culture of undifferentiated human pluripotent stem cells

In the previous chapter, genes selectively upregulated in ΔMet cells were determined from gene array profiling analysis. From the 18 genes, I focused on *SLC30A1*, which encodes a Zn efflux transporter, ZNT1. Also, decreased intracellular protein-bound Zn content was significantly observed in ΔMet pretreated cells, while other metal contents did not change. By culturing undifferentiated PSCs in ΔZn media (Chelex 100), decreased cell number and decreased intracellular Zn content were confirmed. The effect of culturing cells under the ΔZn condition mimics the ΔMet pretreatment effect reported previously (Shiraki et al., 2014).

Therefore, I am interested in further examination of the relationship of Met and Zn in culturing undifferentiated PSCs (Chapter 3) and in cell differentiation (Chapter 4). In chapter 3, to ease the Zn depletion procedure, I introduced a novel custom media, made in collaboration with Ajinomoto Co. Inc. By using this novel media, I aimed to examine the effect of Zn on cell growth, proliferation, and gene expression level of undifferentiated PSCs that were being cultured under various Zn conditions.

Chapter 4: Roles of Zinc in pancreatic differentiation using undifferentiated human pluripotent stem cells

Results from chapter 2 highlighted that ΔMet pretreated PSCs enhance the differentiation, leading to the generation of functional pancreatic β cells that exhibited almost the same level of insulin secretion as those of human islets. Then, by using the novel ΔZn media, the result demonstrated that the absence of Zn in PSCs cell maintenance media triggers the upregulation of cell differentiation markers. This phenomenon is seen under ΔMet pretreatment too. This suggests that molecular mechanisms involving ΔMet and Zn in differentiation potency might be mediated through intracellular Zn contents in cells.

Next, I would like to find out how Zn concentration in media would affect pancreatic differentiation. By using the *in vitro* pancreatic differentiation of undifferentiated PSCs procedure in our lab (refer to Methods), I altered the Zn concentration in the differentiated cell culture media and examined the optimum amount of Zn needed during pancreatic differentiation.

Chapter 5: Relationship between Methionine and Zinc in human pluripotent stem cells

Until now, my results showed that ΔMet pretreatment not only elevates definitive endoderm (DE) differentiation but also increases pancreatic β cell differentiation efficiency. From exploring the gene expression profile of ΔMet cell group, *SLC30A1*, Zn efflux transporter localized on the plasma membrane, was my target. This led me to connect Met and Zn while I study the effect of Zn in maintaining cell proliferation of PSCs and in pancreatic differentiation using PSCs.

In this chapter, I would like to discuss the experiments I have done to try to define the interaction of Methionine (Met) metabolism and Zinc (Zn) signaling in regulating the maintenance and differentiation of PSCs.

Chapter 2: Methionine metabolism regulates maintenance of pluripotent stem cells and differentiation into pancreatic β cells

2.1 Methionine deprivation (ΔMet) pretreatment potentiates late-stage differentiation into pancreatic β cells

To explore if ΔMet pretreatment could potentiate late-stage differentiation into pancreatic β cells, I performed pancreatic differentiation using ΔMet pretreated RPChiPS771 PSCs, following the pancreatic differentiation procedure modified in our lab (refer to Methods). On day 3 DE stage, under ΔMet pretreatment condition, the cells exhibited significantly decreased OCT3/4-positive cell population (Figure 2.1A). On day 25, ΔMet pretreated cells also resulted in an increased INSULIN/PDX1 double-positive cell population (Figure 2.1B). Lastly, I managed to generate functional pancreatic β cells with a stable glucose response insulin secretion (Figure 2.1C). ΔMet pretreated PSCs gave rise to pancreatic β cells, showing a more stable insulin secretion compared to those derived from PSCs culture under Compl medium. Overall, the results concluded that ΔMet pretreatment not only enhances endodermal differentiation but also potentiates the generation of functional pancreatic β cells that exhibited almost the same level of glucose-stimulated insulin secretion as those of human islets.

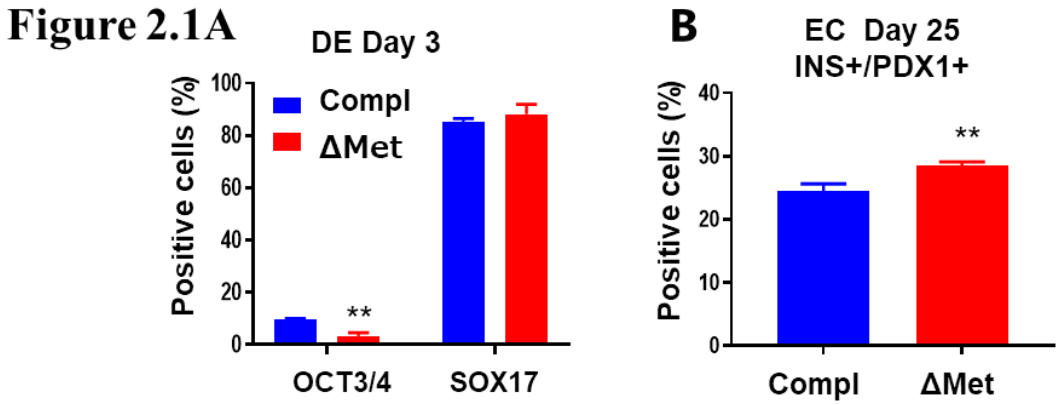

Figure 2.1

A: Day 3 immunocytochemistry analyses showed that ΔMet pretreated cells exhibited decreased OCT3/4-positive cell population.

B: Day 25 immunocytochemistry analyses showing ΔMet pretreated cells increased INSULIN/PDX1 double-positive cell population compared to the control.

Figure 2.1C

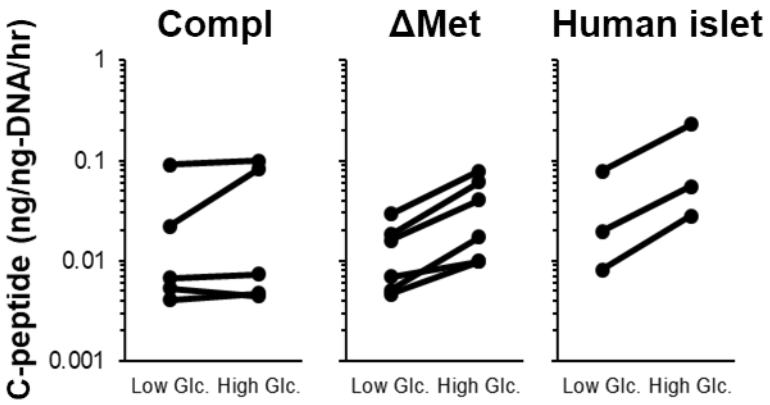

Figure 2.1

C: Glucose-Stimulated Insulin Secretion (GSIS) activity of RPChiPS771 human iPS cell-derived endocrine cells and human islets. Human iPS cell-derived endocrine cells pre-treated with methionine deprivation (middle panel, n=6) showed improved glucose-stimulated c-peptide secretion compared to that of control cells (left panel, Compl, n=5), with a high to low glucose ratio that resembles that of human islets (right panel, n=3).

2.2 Upregulation of *SLC30A1* expression as a target of ΔMet

To investigate the effect of ΔMet in regulating cell differentiation, gene array profiling analysis was performed using RNA extracted from human KhES3 and 201B7 hiPSCs cultured in five hours Complete (Compl) or ΔMet medium (Figure 2.2A). There were 18 genes significantly upregulated across three array sets (Figure 2.2B). *SLC30A1*, which encodes Zn transporter 1 (ZNT1) protein, was one of the upregulated genes selectively in ΔMet pretreated cells compared to controls. Then, the expression levels of genes encoding all Zn transporters, *SLC30A1-10,* and *SLC39A1-14*, were examined using ΔMet, or other amino acids deprivation (ΔAA) pretreatment using RPChiPS771 PSCs. Other amino acids include threonine, valine, ileum, leucine, lysine, histidine, phenylalanine, and tryptophan (Figure 2.2C). *SLC30A1* was significantly upregulated selectively in the ΔMet group. *SLC39A1* was also upregulated but to a smaller degree (> 1.5-fold). On the other hand, *SLC30A5*, *SLC30A6*, *SLC30A7*, *SLC39A6*, *SLC39A8*, and *SLC39A10* expression levels in both ΔMet and ΔAA pretreated cells showed downregulation compared to control (Figure 2.2D).

ZNT1 localizes to the plasma membrane and is the only transporter that delivers Zn ions out of the cell when cellular Zn levels increase (Kimura and Kambe, 2016; Nishito and Kambe, 2019) (Figure 1A). Therefore, it can be implied that the upregulation of ZNTI would theoretically cause decreased intracellular Zn content in cells. To investigate whether intracellular Zn content is affected by ΔMet pretreatment, the contents of intracellular heavy metals Zn, copper (Cu), and Iron (Fe) (labile or protein-bound forms) were measured in undifferentiated RPChiPS771 PSCs treated with ΔMet or ΔAA for 5 hours (Figure 2.2E). The results show a decrease in protein-bound Zn under ΔMet conditions, while other ΔAA conditions do not have any significant reduction. The reduction was significantly observed with protein-bound Zn content but not with labile Zn or other heavy metals (Figure 2.2F).

It is reported that the binding of protein to Zn is mediated through sulfur in the sulfhydryl group of cysteine (Kambe, 2019). A study also suggested that homocysteine (HCY) targets intracellular metallothionein by forming a mixed-disulfide conjugate, releasing free Zn ions into the cytoplasm (Barbato et al., 2007). This fits the results above as ΔMet led to decreased protein-bound Zn content (Figure 2.2E), meaning increasing free Zn ions in cells. In addition, the Kume-Shiraki Lab previously reported that under ΔMet conditions, hPSCs ceased to excrete HCY (Shiraki et al., 2014). This suggests that under the ΔMet condition, a temporal increase in intracellular HCY might occur that caused Zn to be competed out from its binding protein. Several concentrations (1, 5, 10, 50, 500, 1000, or 2000 μM) of HCY

were added to the hiPSC lysates cultured under Compl and ΔMet conditions to prove this hypothesis. Then, the contents of the protein-bound metals (Zn, Cu, Fe) were measured. Protein-bound Zn decreased in proportionate to the increase in HCY addition, from 50 μM, 500 μM, 1 mM to 2 mM. No change was observed in protein-bound Fe and Cu (Figure 2.2G). While under ΔMet condition, as low as 0.5 mM HCY was enough to reduce the protein-bound Zn to a similar level at 2 mM HCY in the Compl condition. The result supports the hypothesis that the cessation of HCY excretion under ΔMet increased intracellular local HCY. Added HCY binds with the binding protein and causes decreased protein-bound Zn. The result suggests that Met metabolism regulates protein-bound Zn level through HCY.

Figure 2.2

A

5 h ΔMet / Compl > 3

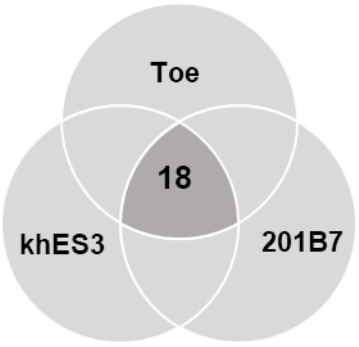

B

ALS2CR12	*amyotrophic lateral sclerosis 2chromosome region, candidate 12*
CBX4	*chromobox homolog 4*
CEBPB	*CCAAT/enhancer binding protein (C/EBP), beta*
CHAC1	*ChaC, cation transport regulator homolog 1*
CSRNP1	*cysteine-serine-rich nuclear protein 1*
CTGF	*connective tissue growth factor*
DDIT4	*DNA-damage-inducible transcript 4*
DHRS2	*dehydrogenase/reductase (SDR family) member 2*
EGR1	*early growth response 1*
FGF21	*fibroblast growth factor 21*
GADD45B	*growth arrest and DNA-damage-inducible, beta*
RGS16	*regulator of G-protein signaling 16*
SESN2	*sestrin 2*
SLC30A1	***solute carrier family 30 (zinc transporter), member 1***
STC2	*stanniocalcin 2*
THBS1	*thrombospondin 1*
TRIB3	*tribbles pseudokinase 3*
ULBP1	*UL16 binding protein 1*

Figure 2.2

A: Gene expression array analyses of pluripotent PSCs treated with ΔMet or control, complete medium was performed with hiPSCs 201B7 (GSE151795) and Toe (GSE151794). The results were compared with previous gene expression array analysis of KhES3 ESCs (GSE55285) (Shiraki et al., 2014).

B: Eighteen genes are commonly upregulated in ΔMet groups. The results identified *SLC30A1* as a gene that was specifically upregulated upon ΔMet treatment, along with 17 other genes.

Figure 2.2

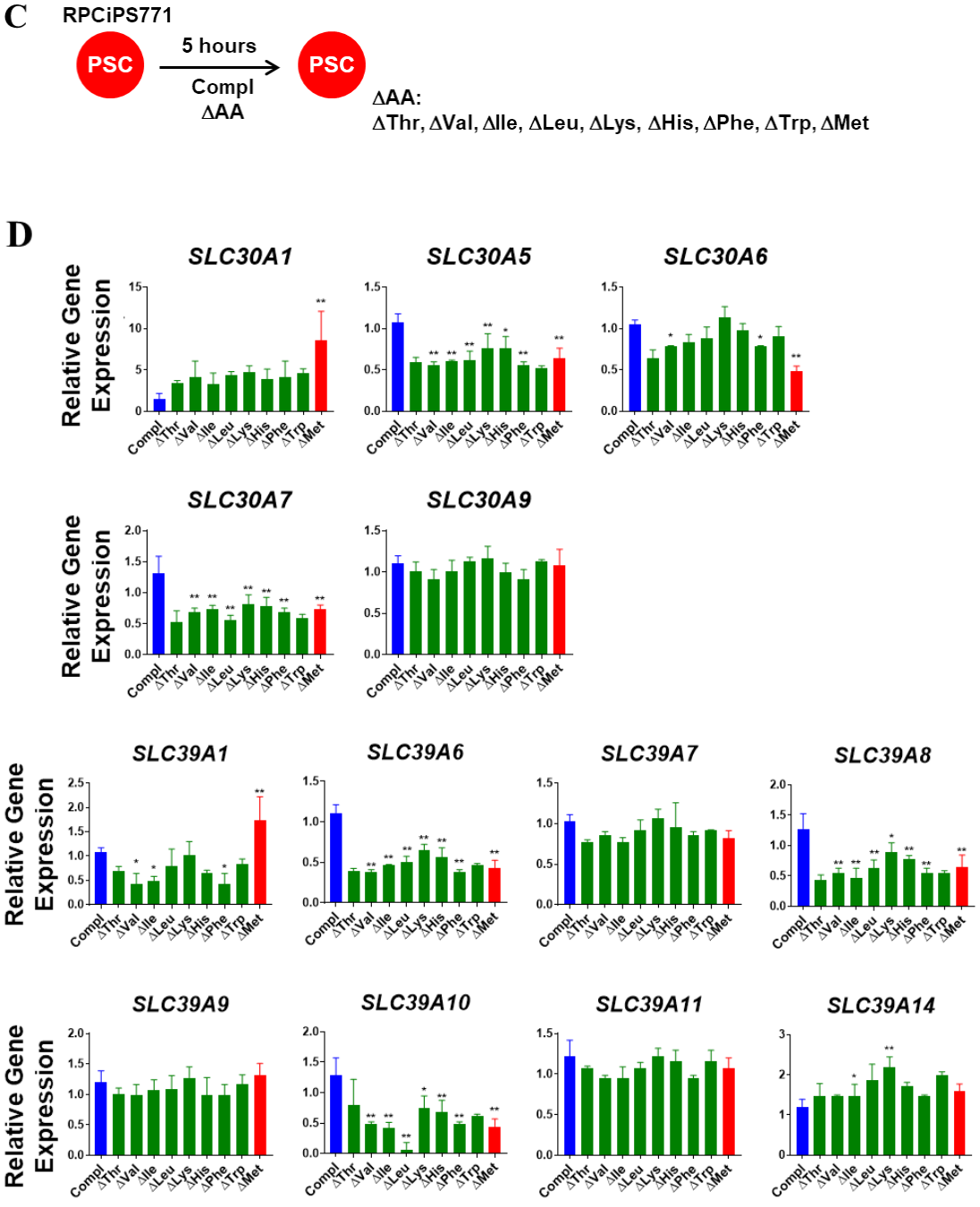

Figure 2.2

C: A schematic diagram showing RPCiPS771 cells being treated with various amino acid deprivation pretreatment before being subjected to real-time PCR analyses.

D: Real-time PCR analyses of the expression of SLC30A and SLC39A genes in pluripotent RPChiPS771 iPSCs upon deprivation of single amino acid. Only SLC30A1 was specifically upregulated upon ΔMet. N=3, excluding ΔThr, ΔTrp (N=2).

Data are expressed as mean ± SD. Differences are shown as *p<0.05, **p<0.01, analyzed by one-way ANOVA Dunnett's multiple comparisons test.

Figure 2.2

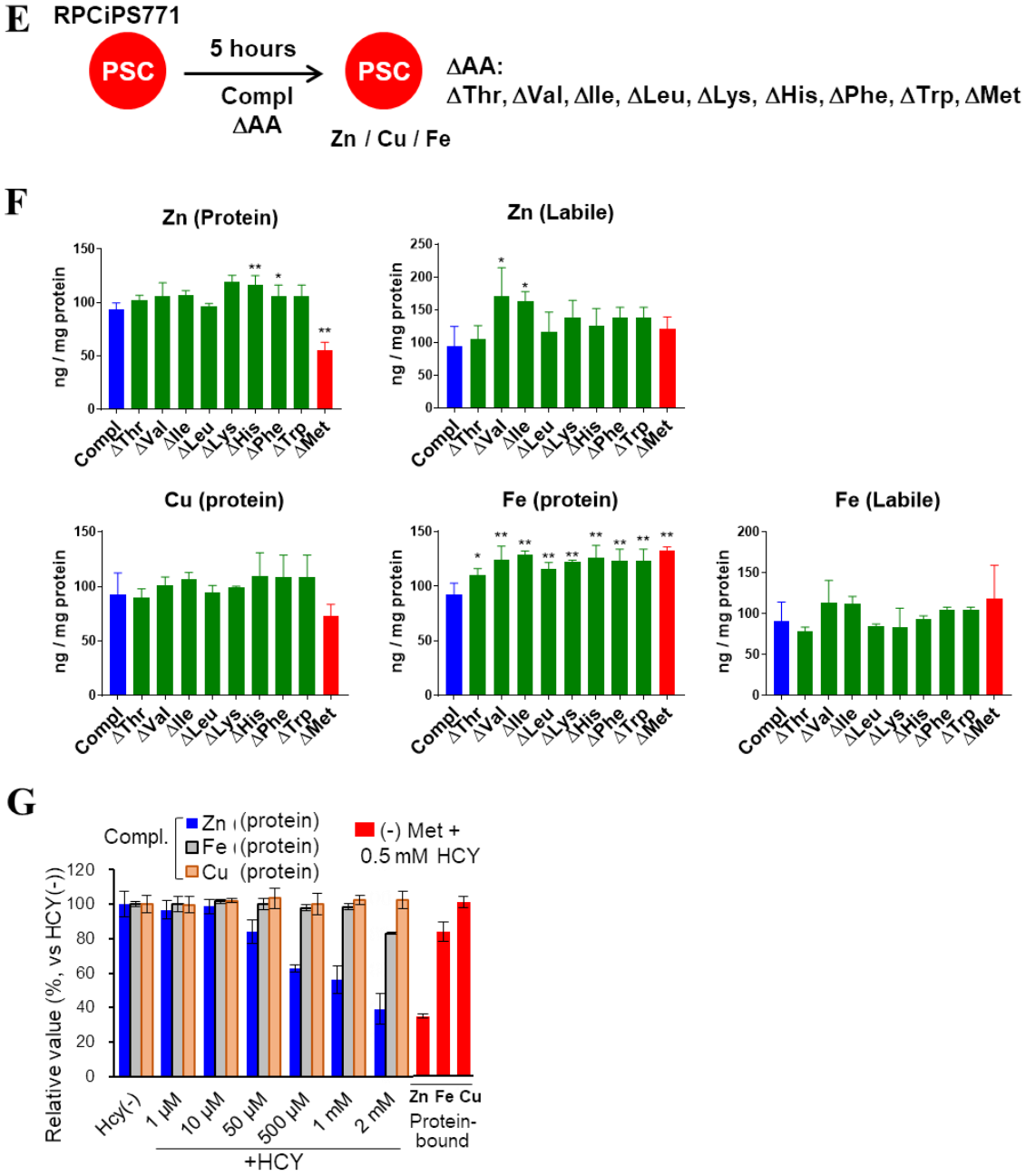

Figure 2.2

E: A schematic diagram showing RPCiPS771 cells being treated with ΔMet or other single Δamino acids for five hours and subjected to analysis of intracellular heavy metal contents of Zn, Copper (Cu), and Iron (Fe).

F: Protein-bound Zn significantly decreased in PSCs cultured under ΔMet, but not in other Δamino acids conditions. Labile-form Zn, Fe, and Cu were not affected by ΔMet.

G: The addition of HCY into Compl cell lysate (blue bar) reduced protein-bound Zn but not other heavy metal contents. In contrast, ΔMet (red bar) required lower HCY to reduce protein-bound Zn.

2.3 Culturing undifferentiated PSCs under Zinc deprived media

Our results indicate that ΔMet pretreatment of undifferentiated PSCs caused a reduction in intracellular Zn content. We then hypothesized that the reduction in intracellular Zn may contribute to the elevation of differentiation potency in ΔMet cells. We tried to reduce intracellular Zn contents by culturing undifferentiated PSCs in Zn-deprived (ΔZn) media. As described in the Methods, ΔZn media is prepared using a chelating reagent, Chelex 100 (Bio-Rad Laboratories, Inc.).

Undifferentiated PSCs were cultured using Control and Chelex (ΔZn) media for 72 hours. The proliferation of ΔZn treated cells was not obvious from 48-hour-culture, while the control cells showed a continuous proliferation from 24 hours to 72 hours (Figure 2.3A). The relative cell number resulted in a drastically decreased cell number in the ΔZn condition while the controls showed doubled relative cell number from 48 to 72 hours (Figure 2.3B). Furthermore, intracellular Zn contents in ΔZn treated cells significantly decreased at 48 and 72 hours compared to controls (Figure 2.3C). Overall, the results suggest that Zn is necessary for PSCs cell growth and that intracellular Zn contents can be altered by changing the Zn concentration added into the cell culture media.

Furthermore, RNA was extracted from 48- and 72-hour Control and Chelex (ΔZn) cultured cells, and real-time PCR was performed. The expression levels of undifferentiated cell markers, *LIN28* (pluripotency marker), *DNMT3B* (*DNA methyltransferase 3B*; embryonic stem cell marker), *TERT* (*telomerase reverse transcriptase*; self-renewal marker), and *ZFP42* (encoding a zinc finger protein; pluripotency marker), did not change much in Controls at 48 or 72 hours. While cells cultured in Chelex (ΔZn), exhibited significantly decreased expressions in each gene compared to Controls. Chelex (ΔZn) cells showed a further decrease in *TERT* and *ZFP42* at 72 hours (Figure 2.3D). For differentiation markers, *EOMES* (*Eomesodermin*; trophoblast), *SOX17* (*SRY-box 17*; definitive endoderm), *CDH5* (*Cadherin 5*; endothelial cell), *GATA4* (*GATA Binding Protein 4*; extra-embryonic endoderm), *ISL1* (*LIM-homeodomain transcription factor Islet 1*; ectoderm), the gene expression levels were upregulated in Chelex (ΔZn) cells, compared to Controls (Figure 2.3E). Gene expression in ΔMet pretreated PSCs was also being examined. Downregulation of genes involved in self-renewal or pluripotency, *DMNT3B* and *TERT*, and upregulation of differentiation marker genes, *EOMES*, *SOX17*, *GATA4*, and *ISL1* were significantly observed in ΔMet pretreated cells, compared to the control (Figure 2.3F).

In Chapter 1.2, I mentioned that ΔMet triggered a decrease in the intracellular protein-bound Zn content level. From this chapter, these results showed that the intracellular Zn

content decreased under Chelex (ΔZn) condition. Also, Chelex (ΔZn) treated cells exhibited reduced undifferentiated cell markers while elevated differentiation marker gene expressions, which is also observed in ΔMet pretreated cells. The similarity in gene expression patterns may suggest that there is a relationship between ΔMet and ΔZn treated PSCs.

Figure 2.3

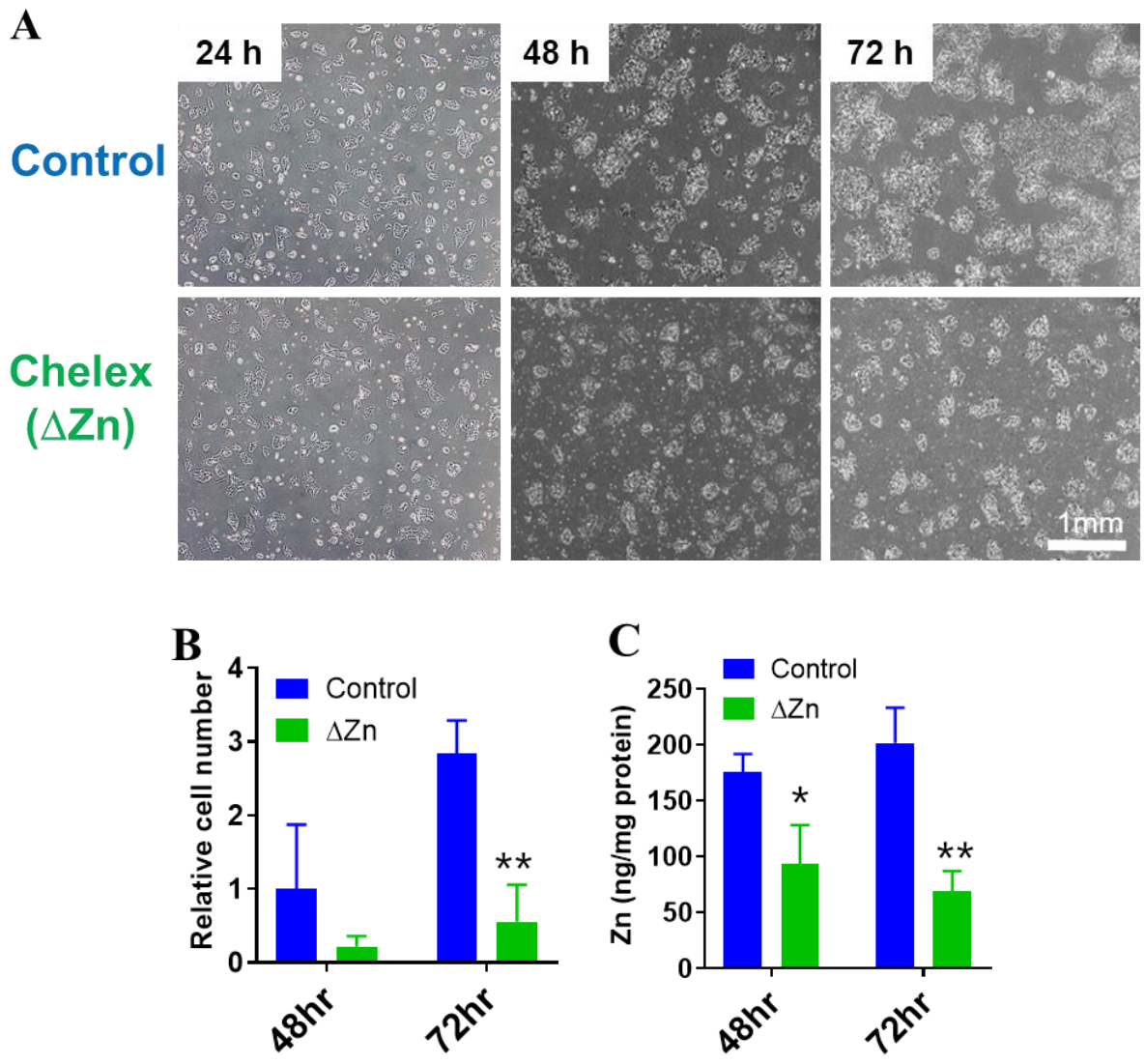

Figure 2.3

A: Bright-field images of undifferentiated RPChiPS771 cells cultured with control or Chelex (ΔZn) medium for 24, 48, or 72 hours.

B: Relative cell number and C: intracellular protein-bound Zn content decreased with increasing culture time under ΔZn.

Figure 2.3

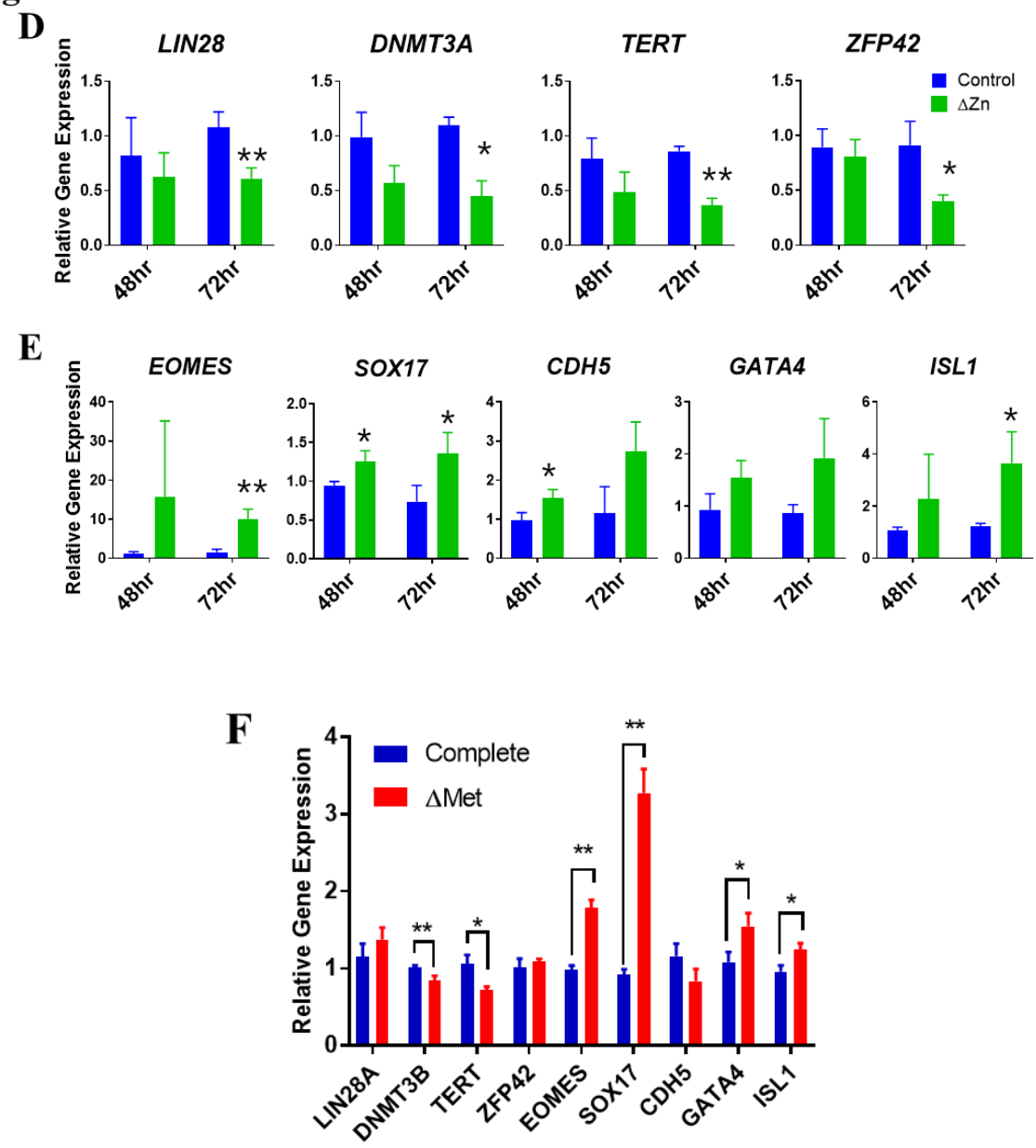

Figure 2.3

D, E: Expression of gene markers for pluripotency and proliferation (D) or differentiation (E) are shown.

F: Expression of gene markers was examined in cells treated with ΔMet for five hours.

Data are expressed as mean ± SEM. N=3. Differences are shown as *p<0.05, **p<0.01, analyzed by a two-tailed unpaired Student's t-test.

2.4 Discussion

Focusing on the differentiation potency of ΔMet pretreatment, I performed pancreatic differentiation comparing Compl and ΔMet pretreated PSCs. As a result, ΔMet pretreatment was shown to promote endodermal and pancreatic differentiation (Figure 2.1A, B). The pancreatic β cells derived from ΔMet pretreated PSCs also showed a more stable glucose-stimulated insulin secretion ability compared to the Compl condition (Figure 2.1C).

Microarray analysis was performed to study the molecular mechanism of differentiation potency of ΔMet to explore common expression profiles among different cell lines. Among the upregulated genes, I focused on *SLC30A1*, which encodes a Zn efflux transporter ZNT1. *SLC30A1* was only upregulated under ΔMet but not the deprivation of other amino acids (Figure 2.2D). Decreased intracellular protein-bound Zn content was also observed in ΔMet pretreated cells while labile Zn and other metals changes were not (Figure 2.2F). The decreased protein-bound Zn content might be caused by a temporal increase in local HCY under ΔMet condition (Figure 2.2G). From the results, I hypothesized that ΔMet pretreatment in PSCs potentiates cell differentiation through Zn signaling involving HCY in the methionine cycle.

As upregulation of *SLC30A1* and decreased intracellular protein-bound Zn content was observed, I thought that reducing the Zn concentration in cell culture could manipulate the reduction of intracellular Zn content, and trigger cell differentiation in PSCs. Therefore, Chelex (ΔZn) media was prepared and used to culture undifferentiated PSCs. The relative cell number drastically decreased under Chelex (ΔZn) condition (Figure 2.3A, B). This phenomenon is similar to that reported in mouse ESCs, as 2 μM of zinc chloride ($ZnCl_2$) transiently maintained mouse ESCs pluripotency *in vitro* (Hu et al., 2016). Another report also demonstrated that the number of mouse ESCs colonies increased monotonically as the extracellular concentration of Zn did (Mnatsakanyan et al., 2019). These results suggest that Zn has an important role in maintaining cell pluripotency of mouse ESCs. And in my thesis, I demonstrated that Zn also maintains cell pluripotency of human iPSCs. Furthermore, the intracellular Zn content was significantly decreased compared to control (Figure 2.3C), suggesting that reducing Zn in cell culture can reduce the intracellular Zn content of PSCs. Overall, the ΔZn condition reduced cell proliferation, decreased intracellular protein-bound Zn, and increased differentiation gene markers in undifferentiated PSCs. This is similar to the effect of ΔMet on undifferentiated PSCs. Therefore, my next step is to study the ΔZn

effect in differentiating PSCs (Chapter 4) and try to determine the relationship between Met and Zn in regulating differentiation potential in PSCs (Chapter 5).

Chapter 3: Roles of Zinc in the maintenance culture of undifferentiated human pluripotent stem cells

3.1 Zn concentration adjustable media in cell culture

StemFit AK03N cell culture media (Ajinomoto Co.) is used for the maintenance culture of undifferentiated PSCs. This medium is xeno-free and has been domestically approved for use in the clinical settings. In an attempt to investigate the optimum Zn amount needed in the maintenance culture of PSCs, our lab collaborated with Ajinomoto and prepared a custom-made basal media without Zn and insulin. By using this media, I can freely adjust the Zn concentration in media and optimize Zn conditions of cell culture using PSCs.

In most of the commercially available culture media, insulin is used as a supplement for sustaining cell growth and self-renewal of PSCs. Insulin molecule is made up of a protein hexamer conjugated to two Zn ions for stabilization. Undifferentiated PSCs maintenance media supplemented with insulin contains approximately 3 μM Zn, hereinafter referred to as undifferentiated AKM (INS) medium. Therefore, instead of using insulin, I made use of insulin-like growth factor (IGF1) as an alternative compound. IGF1, whose molecular structure resembles insulin, is a growth factor that involves vital metabolic regulation and developmental processes in the body (Werner et al., 2008). Another option is APIDRA insulin glulisine (INS*), a rapid-acting insulin analog that does not contain Zn (Becker and Frick, 2008; Garg et al., 2005). Two amino acids, asparagine at position B3 and lysine at position B29, involved in Zn binding are mutated. The structural modifications decrease insulin hexamer formation but stabilize the monomers. The custom-made basal media supplemented with IGF1 or INS* will be referred to as undifferentiated AKM (IGF1) medium or undifferentiated AKM (INS*) medium, respectively. Either medium added with various Zn concentrations, is used to examine the effects of Zn on the maintenance culture of undifferentiated PSCs.

3.2 Cell culture of undifferentiated PSCs under graded Zn concentration conditions

The effect of Zn was first examined by culturing undifferentiated Ff-I01s01 PSCs under 0 μM and 3 μM Zn in undifferentiated AKM (IGF1) and AKM (INS*) (Figure 3A). As mentioned in Chapter 3.1, conventional undifferentiated cells maintenance media usually contain 3 μM Zn, cells cultured under 3 μM Zn condition act as the experimental control.

Under undifferentiated AKM (IGF1)-based 0 μM Zn condition, cell proliferation was not obvious compared to 24 hours. On the other hand, cell proliferation can be confirmed in control as big colony islands were observed at 72 hours under bright field microscopy (Figure 3B). Similar observation can be seen in cells cultured with undifferentiated AKM (INS*) basal medium as control showed increased cell proliferation, while the 0 μM Zn condition exhibited smaller cell colonies at 72 hours of culture (Figure 3C).

Next, undifferentiated Ff-I01s01 PSCs were cultured for 3 days in 8 graded Zn concentration (0, 0.1, 0.3, 0.5, 1, 3, 5, 10 μM) added undifferentiated AKM (IGF1) media. The cells were sampled for EdU incorporation and real-time PCR analysis (Figure 3D). Incorporation of EdU was performed to quantify cell proliferation. Cells cultured under lower Zn concentration, in 0, 0.1, 0.3 and 0.5 μM Zn, exhibited lower relative cell count (DAPI+ cells) compared to control (Figure 3E). EdU positive cell population also significantly decreased in lower Zn concentration (0, 0.1, and 0.3 μM) in comparison to control (Figure 3F). A significantly lesser EdU-positive stain was confirmed under the 0 μM Zn condition (Figure 3G), indicating a reduced cell renewal rate compared to the control.

Furthermore, real-time PCR analysis was performed to examine the gene expression levels of undifferentiated PSCs under undifferentiated AKM (IGF1 + 0, 0.5, 1, 3 μM Zn) or undifferentiated AKM (INS* + 0, 0.5, 3 μM Zn). In undifferentiated AKM (IGF1 + 0 μM Zn) condition, the cells significantly expressed lower levels of cell survival and proliferation genes, *HCK* (*hemopoietic cell kinase*) and *GRB7* (*growth factor receptor-bound protein 7*) compared to control (Figure 3H). Stem cell maintenance genes, *NANOG* and *POU5F1* (also known as *OCT3/4*) did not show significant changes in each condition. On the other hand, differentiation marker genes, *GATA4*, *PECAM1* (*Platelet Endothelial Cell Adhesion Molecule*), and *PAX6* (*Paired box protein PAX6*) were significantly upregulated under 0 μM Zn cells compared to controls (Figure 3I). Downregulations of *HCK* and *GRB7* and upregulations of *GATA4*, *PECAM1* and *PAX6* were also observed in undifferentiated AKM (INS* + 0 μM Zn) condition (Figure 3H, I).

Overall, the results indicate that Zn is necessary for cell proliferation of undifferentiated PSCs. Low Zn (0 μM Zn) downregulates pluripotency and cell renewal markers while upregulated differentiation markers. This is a similar phenomenon observed after PSCs were subjected to five hours of ΔMet pretreatment.

Figure 3

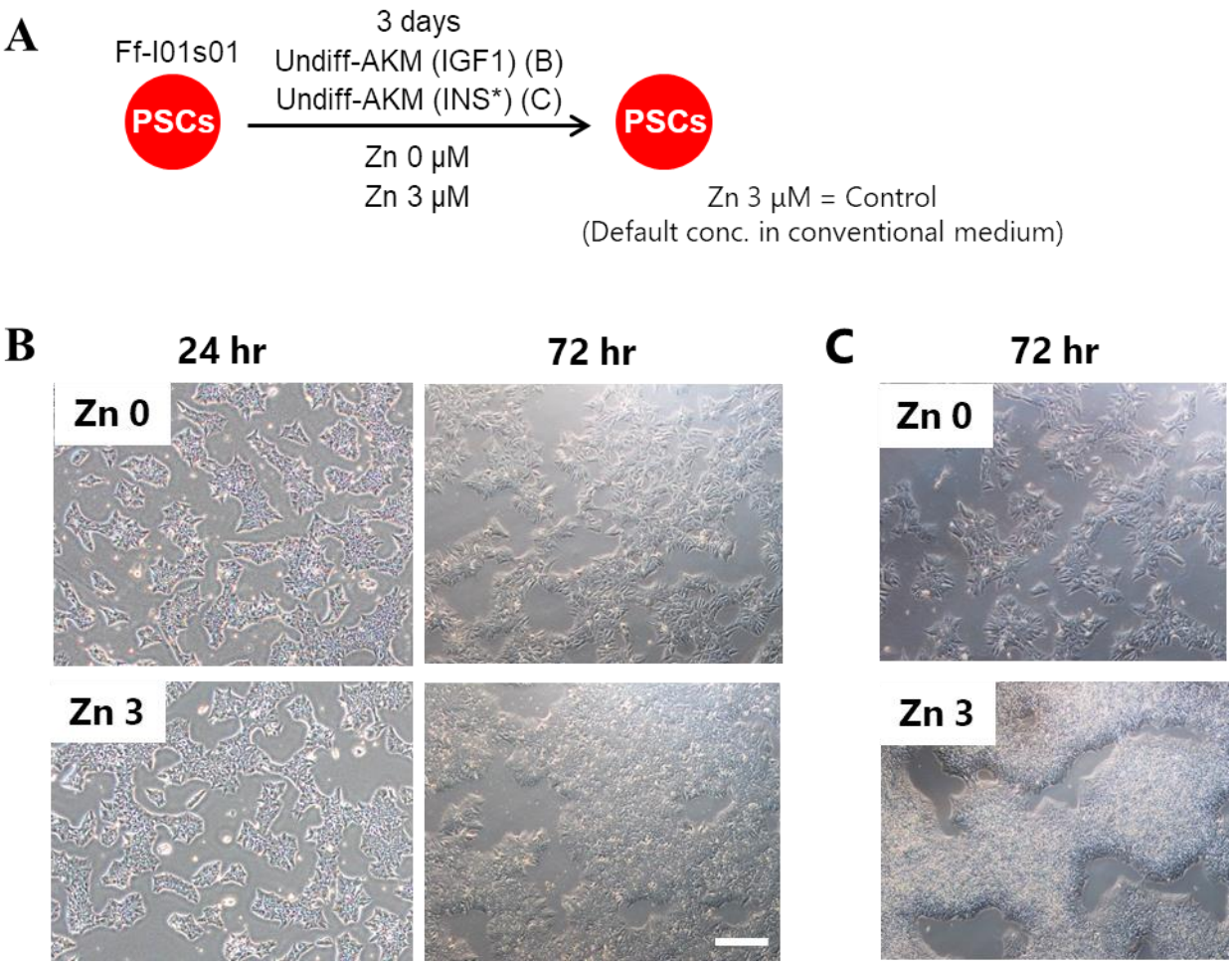

Figure 3

A: A schematic drawing of the experimental design to examine the impact of graded Zn concentrations.

B: Bright-field images of undifferentiated Ff-I01s01 cells cultured with Undiff-AKM (IGF1) based Zn 0 μM or 3 μM medium for 24 or 72 hours.

C: Bright-field images of undifferentiated Ff-I01s01 cells cultured with Undiff-AKM (INS*) based Zn 0 μM or 3 μM medium for 72 hours.

Figure 3

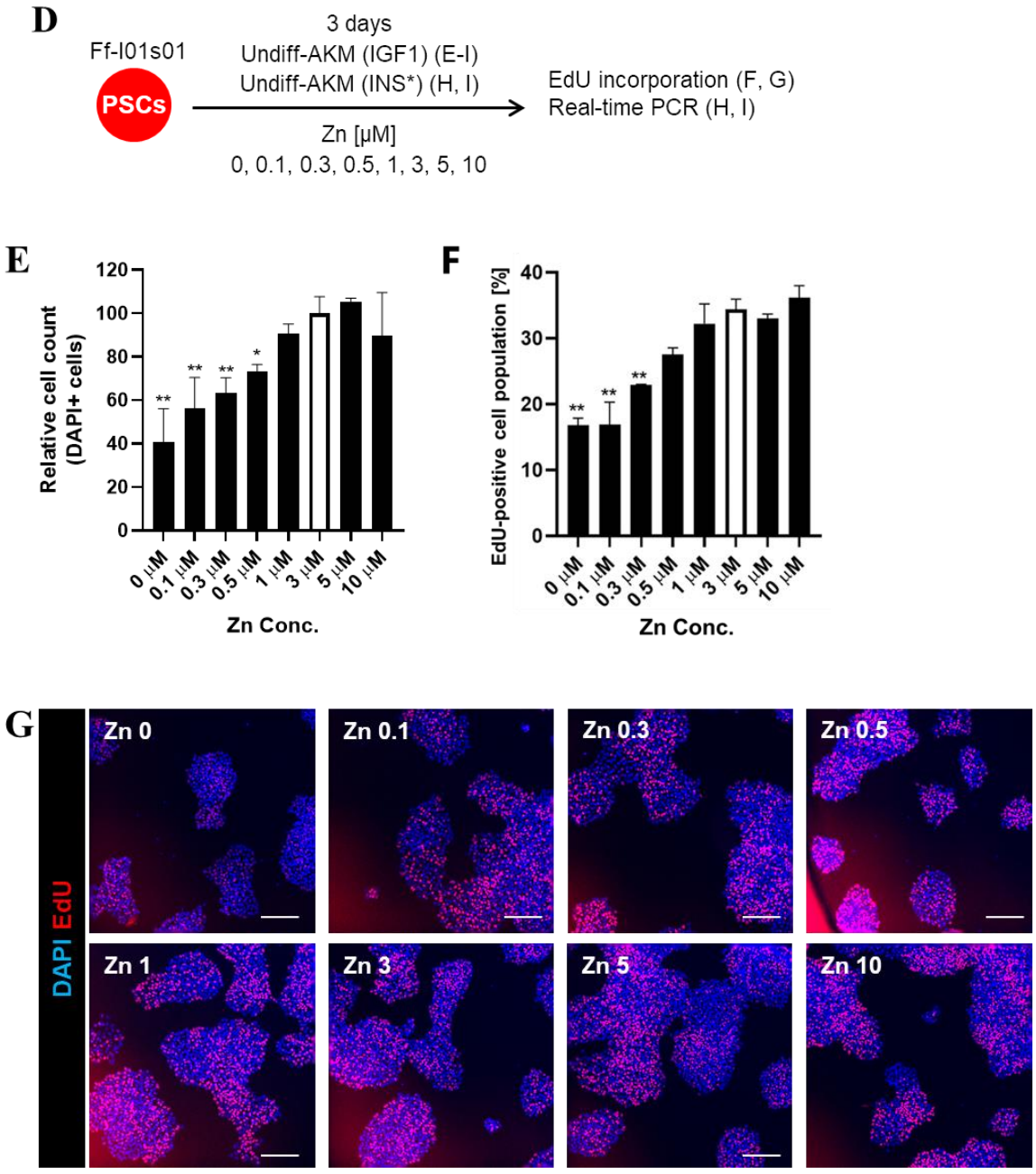

Figure 3

D: A schematic drawing of the experimental to examine the impact of graded Zn concentrations on cell proliferation (E, F, G) and gene expressions (H, I).

E: Relative cell count represented by DAPI-positive cell number. Zn 3 μM as control, represented by 100 (white bar).

F: Edu-positive cell population. Zn 3 μM represents control in the white bar.

G: Immunocytochemical stain results of undifferentiated PSCs cultured under graded Zn concentration conditions. Blue: DAPI, Red: EdU. Scale bar: 200 μm.

Figure 3

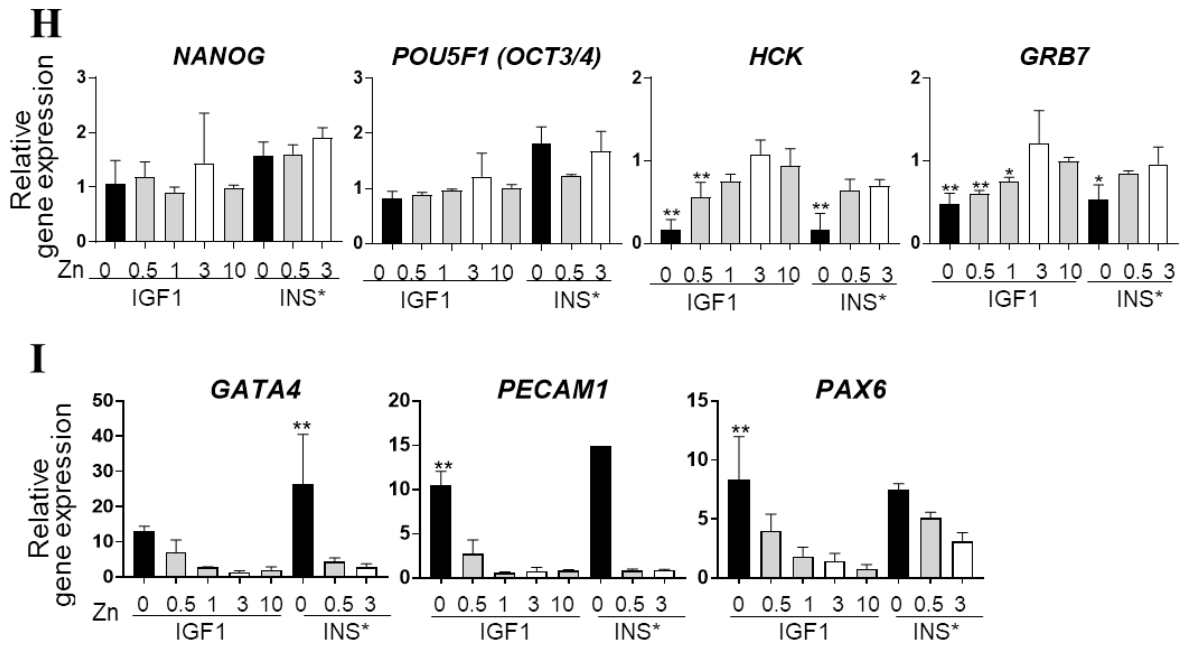

Figure 3

H: Gene expression of pluripotency and cell proliferation gene markers, *NANOG*, *POU5F1* (*OCT3/4*), *HCK*, and *GRB7* were analyzed in Ff-I01s01 PSCs cultured under AKM (IGF1) + bFGF at 5 different Zn concentrations or AKM (INS*) + bFGF at 3 different Zn concentrations for 3 days.

I: Gene expression of differentiation gene markers, *GATA4*, *PECAM1* and *PAX6* were analyzed in Ff-I01s01 PSCs cultured under AKM (IGF1) + bFGF at 5 different Zn concentrations or AKM (INS*) + bFGF at 3 different Zn concentrations for 3 days.

Data are expressed as mean ± SD. N=3. Differences between groups were analyzed by one-way ANOVA Dunnett's multiple comparison test; significances are shown as *$p < 0.05$, **$p < 0.01$, as compared to the 3 μM Zn control condition.

3.3 Discussion

Collaborating with Ajinomoto Co., Zn and INS deprived basal medium is made and can be applied to the maintenance culture of undifferentiated PSCs. INS is removed because INS hexamer often contains excess Zn ions for stabilization. By removing both Zn and INS in culture media, desired Zn concentration can be added for culture considerations. As a substitution of INS, I used insulin-like growth factor (IGF1) and APIDRA insulin glulisine (INS*) as supplements. Both did not contain Zn ions which will not alter the Zn concentration after addition while providing their roles in sustaining cell growth during cell culture.

Undifferentiated PSCs are shown to be able to survive under undifferentiated AKM (IGF1/Zn3) and undifferentiated AKM (INS*/Zn3) media, suggesting the applicability of this custom-made media. The medium added with 3 μM Zn condition act as the experimental control as the Zn concentration in the conventional cell culture media. The cells also showed similar cell morphology compared to undifferentiated AKM (INS). Then, IGF1- or INS*-supplemented undifferentiated culture media was used to examine the effect of Zn. Undifferentiated cells showed decreased cell proliferation at 72 hours under undifferentiated AKM (IGF1/Zn0) and undifferentiated AKM (INS*/Zn0) compared to control. Also, cells cultured in the Zn0 condition exhibited lower relative cell count and cell proliferation, compared to controls, suggesting that decreased Zn concentration in medium affects cell proliferation and Zn is needed for cell growth. Zn0 cells exhibited downregulated cell renewal genes and upregulated cell differentiation genes compared to control. This result is slightly different from the results obtained in Chapter 2.4 using Chelex (ΔZn) media, in terms of the specific gene changes. Undifferentiated PSCs cultured in Chelex (ΔZn) media also expressed downregulated undifferentiated and upregulated differentiation genes. However, the downregulated genes were *LIN28*, *DNMT3A*, *TERT*, and *ZFP42* (Figure 2.3D). These genes did not show apparent downregulations in undifferentiated AKM (IGF1) cultured cells (data not shown). Also, the upregulated differentiation genes in Chelex (ΔZn) were *EOMES*, *SOX17*, *CDH5*, *GATA4*, and *ISL1* (Figure 2.3E). Among these genes, only GATA4 showed a significant increase in 0, 0.5, and 1 μM Zn-undifferentiated AKM (IGF) or (INS*) cultured cells.

The supplements used in both media, AKM (INS) and AKM (IGF1) are INS and IGF1, respectively. Although the concentration of IGF1 added in AKM (IGF1) was known, the concentration of INS in AKM (INS) was unclear. Here, I hypothesized that INS and IGF1 might be the key reason that cells cultured in AKM (IGF1) showed a gene expression

profile slightly different from those cultured in Chelex (ΔZn). As Chelex (ΔZn) medium is made from removing Zn ions in AKM (INS) medium, INS is used as the supplement. Therefore, further investigations involving the activities of INS and IGF1 receptors during cell culture might be needed to study their behavior in cells.

Chapter 4: Roles of Zinc in pancreatic differentiation using undifferentiated human pluripotent stem cells

4.1 Effect of Zn in definitive endoderm (DE) differentiation

Definitive endoderm (DE) differentiation was performed using undifferentiated Ff-I01s01 PSCs. For the differentiation procedure in Kume & Shiraki lab, undifferentiated PSCs were formed into cell spheroids before initiation of differentiation (detailed conditions refer to Methods). After sphere formations, the cell spheroids were treated with five hours of Compl or ΔMet media. Then the cells were cultured in M1-AKM (IGF1) supplemented with 0, 0.5, 3 μM Zn concentrations, while 3 μM stands as a control (Figure 4.1A).

The cell differentiation culture was performed for three days, and cell spheroids were sampled for immunocytochemistry analysis. Undifferentiated cell marker, OCT3/4, and definitive endoderm marker, SOX17, were used as the protein marker. In Compl cells, 0 μM Zn cells had the highest proportion of SOX17-positive cells, almost 90%. While 3 μM Zn cultured cells exhibited approximately 50% OCT3/4-positive cell population (Figure 4.1B). In cells pretreated with ΔMet, the Zn concentration did not seem to affect the DE differentiation. The SOX17 positive cell population was 90% or above among the three Zn conditions in ΔMet pretreated cells (Figure 4.1B). These results suggested that Zn addition (3 μM) affects differentiation efficiency into DE cells.

Next, I sought the timing of Met and Zn contributes to DE differentiation efficiency. Undifferentiated PSCs were subjected to five hours of Compl and ΔMet pretreatment before being differentiated in DE under 0 and 3 μM Zn conditions (Figure 4.1C). The differentiating cells were collected on days 1, 2, and 3. The immunocytochemistry assay with OCT3/4 and SOX17 was then performed. Under Compl and 0 μM Zn condition, the OCT3/4-positive cell population decreased gradually from day 1 and almost disappeared at day 3, accompanied by an increase in the SOX17-positive cell population. A similar result was observed in 3 μM Zn. However, the increased proportion of OCT3/4-positive cells remained until day 3. In ΔMet conditions, decreased percentage of OCT3/4-positive cells was observed starting at day 2 with an increasing SOX17-positive cell population (Figure 4.1D). Overall, ΔMet pretreatment promotes SOX17 expression starting from day 2, while the Zn effect was observed on day 3 of the differentiation.

Furthermore, DE differentiation using eight undifferentiated PSCs cell lines derived from HLA homozygote donors is performed (Figure 4.1E). The cells were cultured for three days in M1-AKM (INS). On day 3, immunocytochemistry was performed with OCT3/4 and

SOX17. There was a big variance in the OCT3/4- and SOX17-positive cells population. For Ff-I01s01 and Ff-I01s04, the percentages of the OCT3/4-positive cells were lower than 20%. While the other cell lines showed a high proportion of OCT3/4-positive cells, exceeding 40%, Ff-I01s01 and Ff-I01s04 cell lines showed a proportion of 60% and above SOX17-positive cells (Figure 4.1F). The results demonstrated that DE differentiation efficiency might differ among cell lines. Therefore, I carried out another DE differentiation using the 0 μM Zn condition, attempting to eliminate the cell line differences. The same cell lines were used and were cultured for three days for DE differentiation. On day 3, immunocytochemistry was performed. Among the eight cell lines, all cells had a 90% and above SOX17 positive cells population. In Ff-MH09s01, Ff-MH15s01, Ff-MH15s02, and Ff-MH23s01 cell lines, there were less than 10% of OCT3/4 positive cells population (Figure 4.1G). The differentiation efficiency is improved compared to Figure 4.1F, in which cells were cultured in M1-AKM (INS). The results suggested that DE differentiation was promoted at 0 μM Zn cell culture conditions, eliminating cell line differences.

Figure 4.1

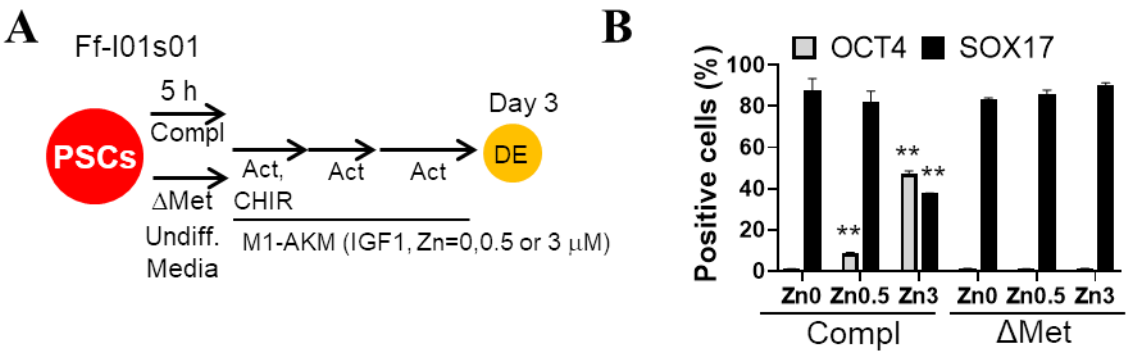

Figure 4.1

A: A schematic diagram showing Ff-I01s01 cells treated with five hours of Compl and ΔMet media, then cultured in M1-AKM (IGF1) supplemented with 0, 0.5, 3 μM Zn concentrations.

B: Immunocytochemistry analysis of day 3 DE cells.

Grey bar: OCT3/4, Black bar: SOX17 positive cells (%)

Data are expressed as mean ± SEM. N=3. Differences are shown as **p<0.01, analyzed by a two-tailed unpaired Student's t-test.

Figure 4.1

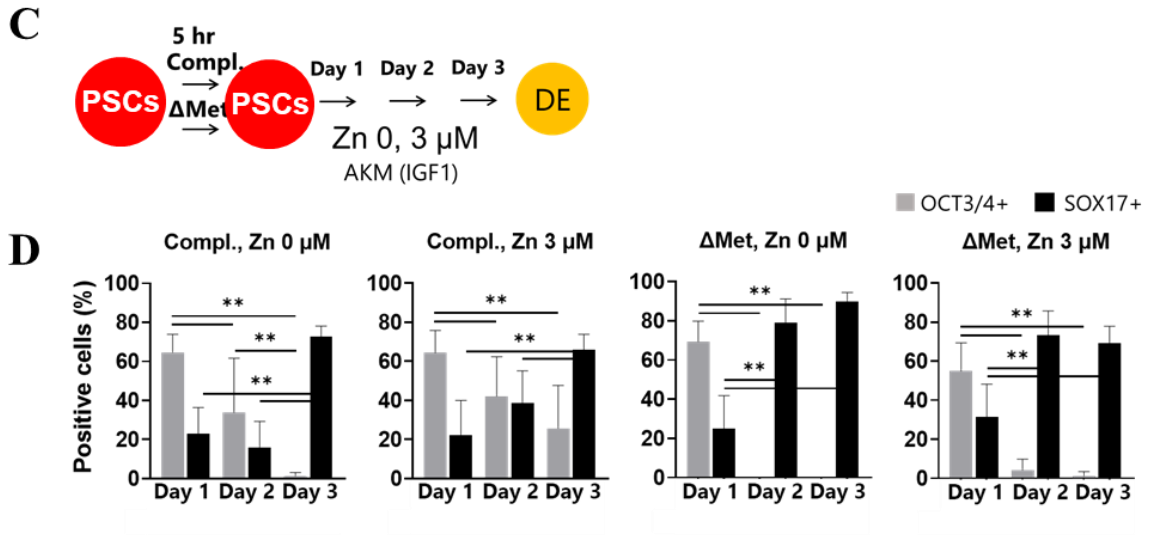

Figure 4.1

C: Schematic diagram showing Ff-I01s01 cells treated with five hours of Compl and ΔMet media and subjected to M1-AKM (IGF1) supplemented with 0, 3 μM Zn. Cells were collected on day 1, 2, and 3 for immunostaining.

D: Immunocytochemistry analysis of day 1, 2, and 3 cells cultured under Compl and ΔMet media, combination with 0 and 3 μM Zn.

Grey bar: OCT3/4, Black bar: SOX17 positive cells (%)

Data are expressed as mean ± SEM. N=3. Differences are shown as **p<0.01, analyzed by a two-tailed unpaired Student's t-test.

Figure 4.1

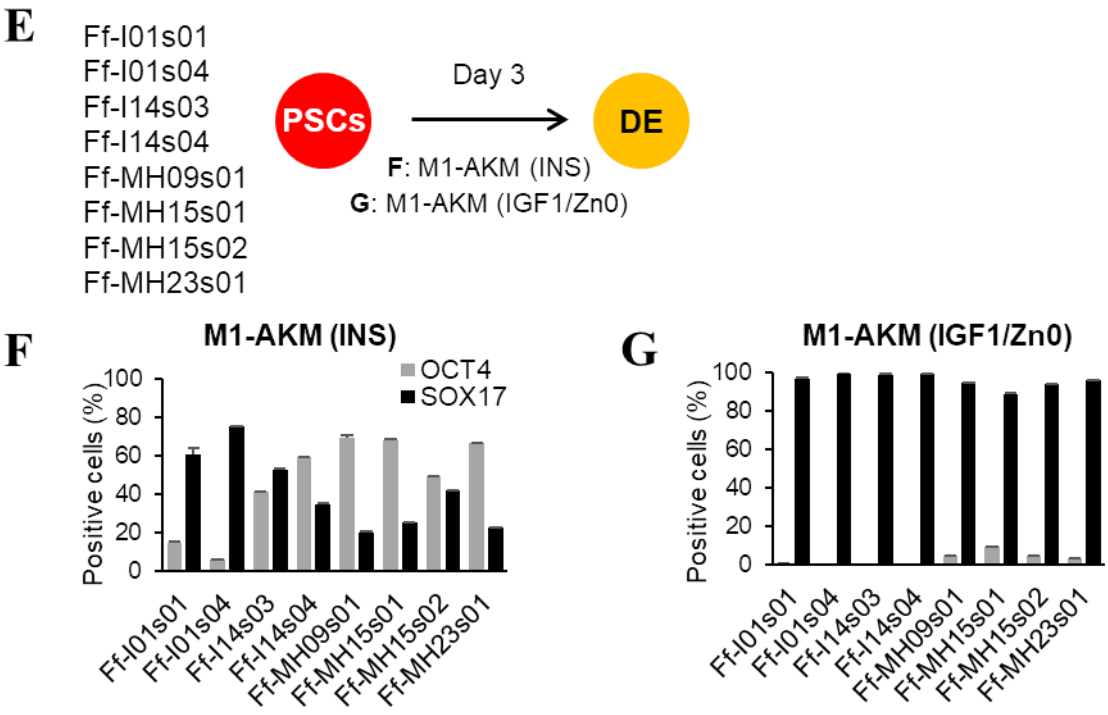

Figure 4.1

E: Schematic diagram of DE differentiation using eight undifferentiated PSCs lines, derived from HLA homozygote donors.

F: Day 3 immunocytochemical stain results of cells cultured under M1-AKM (INS).

G: Day 3 immunocytochemical stain results of cells cultured under M1-AKM (IGF1/Zn0).

4.2 Effect of Zn in differentiation protocol of pancreatic progenitor (PP) to endocrine cell (EC)

Adapting the differentiation procedure described in the previous chapter, undifferentiated PSCs were cultured with M1-AKM (IGF1/0 μM Zn) for DE differentiation. Then, for the later stages of pancreatic differentiation: pancreatic progenitor (PP), endocrine progenitor (EP) and endocrine cell (EC), AKM (IGF1) basal media with 0, 3, 10 μM were used to induce differentiation (Figure 4.2A). However, the cells decreased rapidly following the days of differentiation from day 8 (PP stage), day 13 (EP stage), and then day 20 (EC stage) (Figure 4.2B). On day 20, the cells were too few for further culture and therefore, the culture was terminated. As no big difference in cell numbers and cell morphology was observed during the culture, I suspected the supplement used during differentiation as IGF1 and INS were components to maintain cell growth in culture. Then, I tried to culture cells using AKM (INS*) basal medium. As a result, cells managed to survive until day 20. Compared to IGF1 (Figure 4.2B), more cells were observed in INS* (Figure 4.2C).

To quantify the cell amount changes observed in cell culture plates, cells at day 13 (EP stage) and day 19 (EC stage) were collected for cell count and immunocytochemistry analysis. In Figure 4.2D, the take rate represents the total number count of cells collected at day 13 or day 19 compared with the cell density seeded at the start of differentiation. IGF1-supplemented condition exhibited reduced EP (day 13) cell number to lower than 100% and further lower EC (day 19) cell number on day 19 compared to INS*. The addition of INS* to the IGF1 condition rescued the low cell number of EP (day 13) and EC (day 19). Immunocytochemical results show the proportion of pancreatic progenitor marker, PDX1-positive cell population on day 13 or β cell marker, INSULIN-positive cell population. Both markers did not show any differences between INS* and IGF1-supplemented conditions (Figure 4.2F). Then, I compared the effects of Zn concentration at AKM (INS*/0 or 3 μM Zn) to differentiate PP cells into EP cells (Figure 4.2E). Cells cultured under 3 μM Zn showed a higher percentage in pancreatic marker, NKX6.1-positive cells, more than 50% among PDX1-positive cell population at day 13 (EP cells) compared to 0 μM with approximately 20% positive cell population (Figure 4.2G). Overall, the results suggested that INS supplementation is required for cell survival during the differentiation of PP into ECs. Although IGF1 did not affect pancreatic differentiation, it was not sufficient to support cell growth in my differentiation procedure. Also, instead of 0 μM Zn, 3 μM of Zn concentration in AKM (INS*) basal medium led to efficient differentiation into EP cells, suggesting the impact of Zn addition in pancreatic differentiation.

Figure 4.2

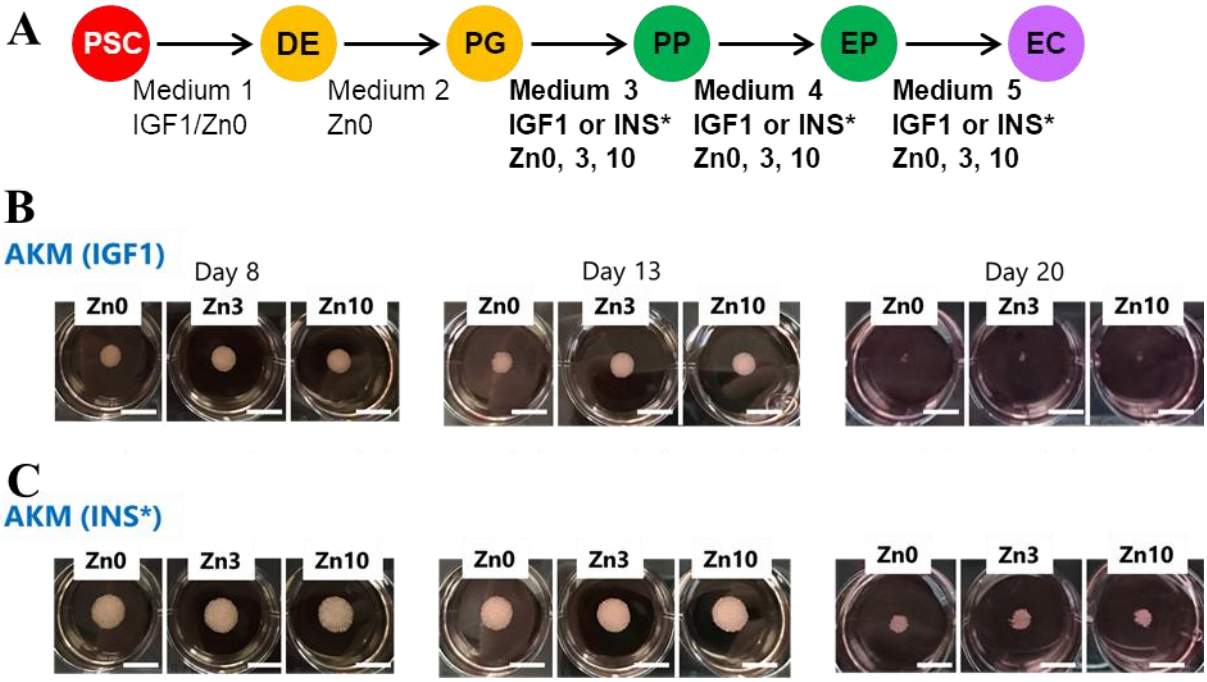

Figure 4.2

A: A schematic diagram representing the pancreatic differentiation procedure, together with the supplements added during each stage for considerations.
PSC: pluripotent stem cell, DE: definitive endoderm, PG: primitive gut tube, PP: pancreatic progenitor, EP: endocrine progenitor. EC: endocrine cell

B: Images of cell spheroids cultured in 6-well-plate (Greiner) at day 8, day 13, and day 20 under AKM (IGF1) basal media supplemented with 0, 3, and 10 μM Zn. Scale bar: 10 mm

C: Images of cell spheroids cultured in 6-well-plate (Greiner) at day 8, day 13, and day 20 under AKM (INS*) basal media supplemented with 0, 3, and 10 μM Zn. Scale bar: 10 mm

Figure 4.2

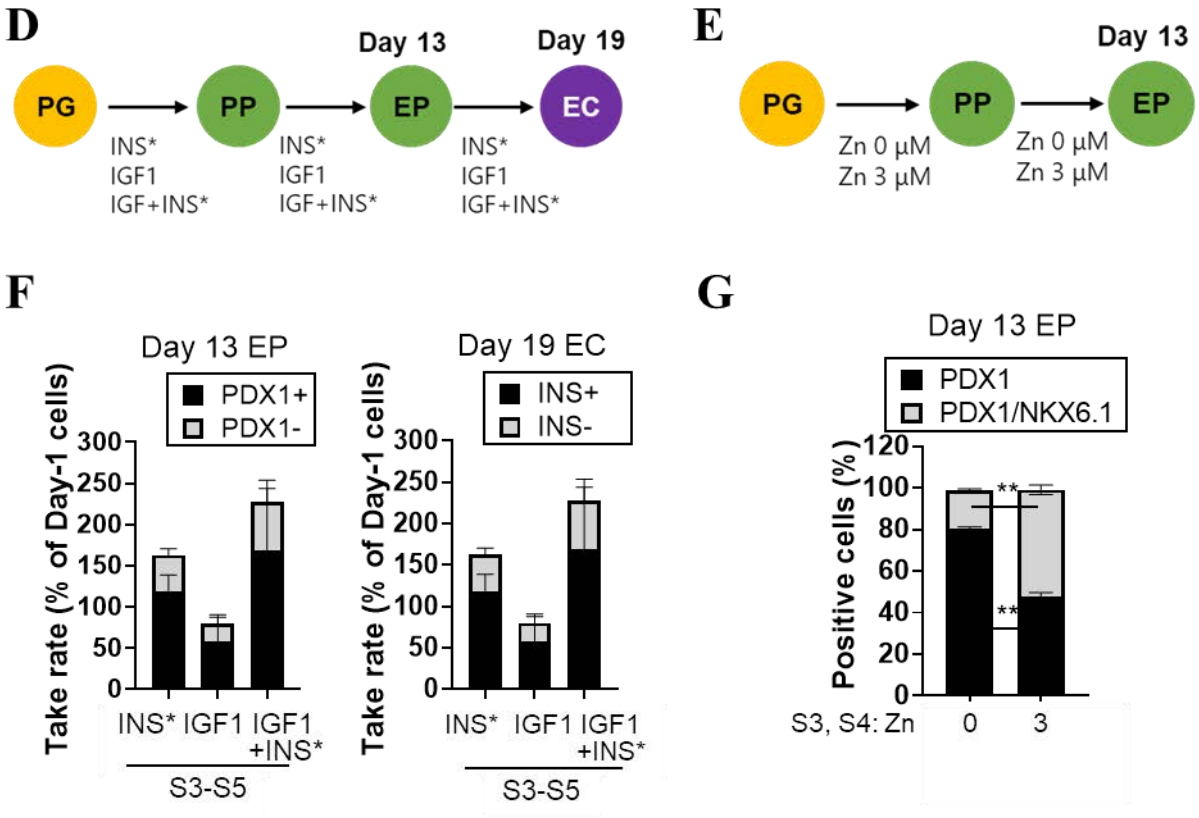

Figure 4.2

D: Schematic diagram showing the later-stage differentiation protocol and conditions of supplements at each stage.

E: Schematic diagram showing the later-stage differentiation protocol with two Zn conditions (0 and 3 μM) at each stage.

F: Yield of day 13 EP and day 19 EC were concluded. Y-axis represents the take rate, which is the total cell count of cells comparing with the cell density at the starting of differentiation. The percentage of PDX1 and INS cells was included in the bar chart.
Day 13 EP; Black bar: PDX1+, Grey bar: PDX1-; Day 19 EC; Black bar: INS+, Grey bar: INS- cells

G: Immunocytochemical staining of PDX1 and NKX6.1 were performed using day 13 EP cells. Black bar: PDX1+, Grey bar: PDX1+/NKX6.1+

Data are expressed as mean ± SEM. N=3. Differences are shown as **p<0.01, analyzed by a two-tailed unpaired Student's t-test.

4.3 PSC-derived functional pancreatic β cells generated under ΔMet and ΔZn procedure

My results in Chapters 4.2 and 4.3 concluded that a brief five hours ΔMet treatment in combination with IGF1-supplemented 0 μM Zn condition during DE differentiation is effective in reducing OCT3/4-positive cell population and generating a high percentage of SOX17-positive cells. Also at the later differentiation stages, INS* supports cell survival better than IGF1 and 3 μM of Zn resulted in a higher population of EP cells. Therefore, by adopting this optimized procedure (Figure 4.3A), pancreatic β cell differentiation was performed using undifferentiated PSCs.

Immunocytochemical analysis was performed using cells collected from each stage: day 3 (DE), day 8 (PP), day 13 (EP), day 21 (EC), and day 33 (pancreatic β cell) to check the differentiation efficiency. Cells were stained with each stage-specific gene marker as shown in Figure 4.3B. On day 3, there were over 99% of SOX17-expressing DE cells. Over 92% of the PDX1-positive cell population was observed on day 8. NKX6.1-expressing EP cells marked 48.8% of the overall cell population on day 13. Lastly, 79.6% INSULIN-expressing EC on day 21 and 73.1% of INSULIN-expressing pancreatic β cells on day 33 were obtained (Figure 4.3C). The pancreatic β cell sphere derived from PSCs on day 33 showed an islet-like structure compared with human islet morphology (Figure 4.3D).

Next, a glucose-stimulated insulin secretion assay was performed to examine the functionality of PSC-derived pancreatic β cells and human islets as control. The results showed that day 39 pancreatic β cells responded to high glucose (20 mM) and showed glucose-stimulated insulin secretion similar to that observed in human islets (Figure 4.3E). The results demonstrated that the ΔMet and ΔZn procedure is applicable for the generation of pancreatic β cells with a high INSULIN-expressing cell population and the capability of glucose-stimulated insulin secretion activity.

Figure 4.3

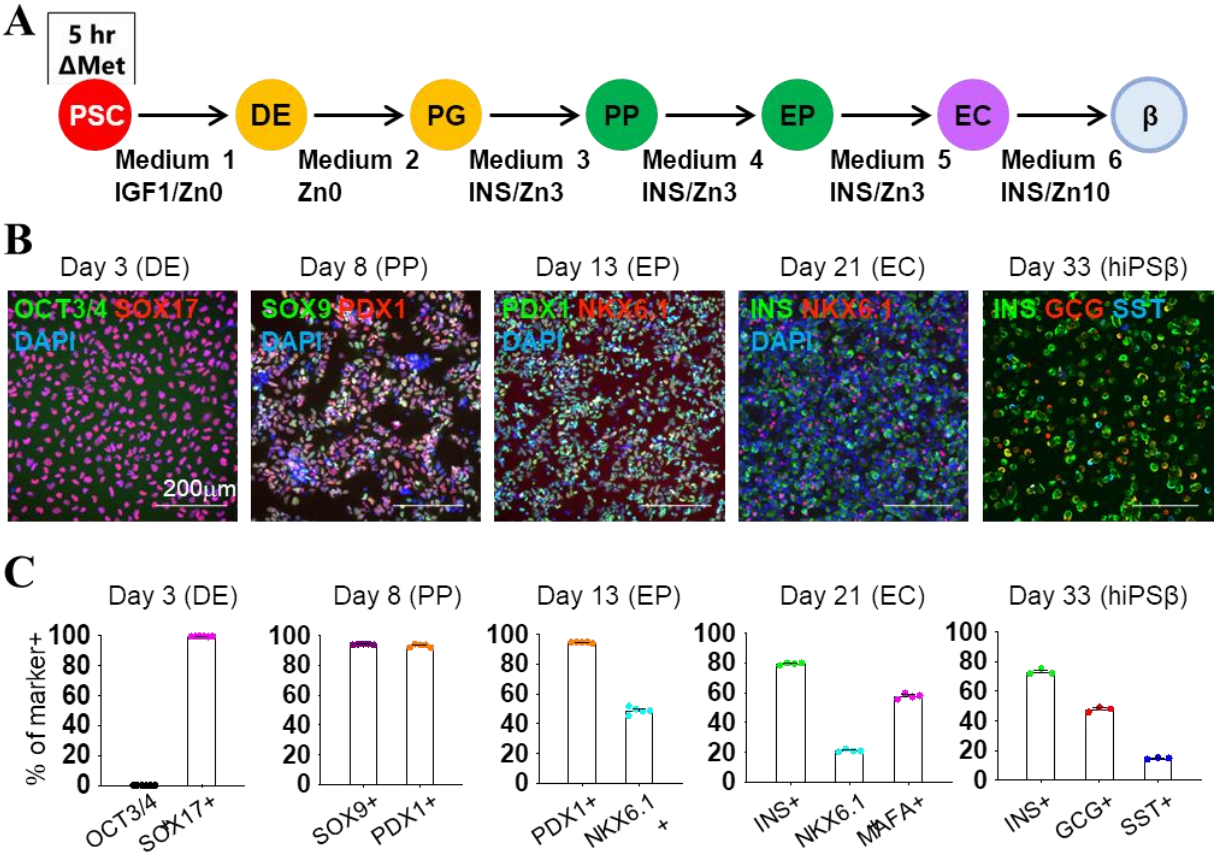

Figure 4.3

A: A schematic diagram showing ΔMet and ΔZn applied pancreatic differentiation procedure. PSC: pluripotent stem cell, DE: definitive endoderm, PG: primitive gut tube, PP: pancreatic progenitor, EP: endocrine progenitor. EC: endocrine cell

B: Immunocytochemistry analysis of marker expression on day 3 DE, day 8 PP, day 13 EP, day 21 EC, and day 33 human PSC-derived β cells are shown. Scale bar: 200 μm

C: Quantitative analyses of B) are shown. OCT3/4 (green), SOX17 (red), SOX9 (green), PDX1 (red), NKX6.1 (red), INS (green), glucagon (GCG; red), and nuclei (DAPI, blue).

Figure 4.3

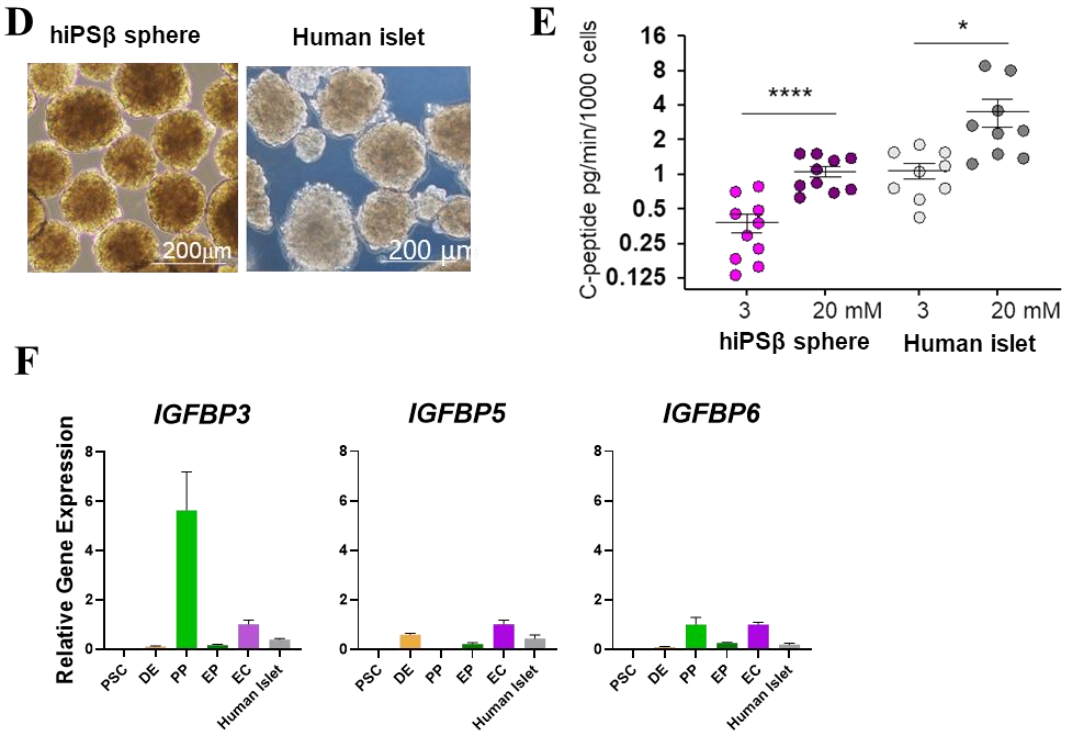

Figure 4.3

D: Bright-field images of human PSC-derived β cells (right) and human islets (left) are shown. Scale bar: 200 μm

E: Glucose-stimulated insulin secretion activities assayed on day 39. Normalized C-peptide measurements in response to low glucose (LG, 2.5 or 3.0 mM; pink, light gray) and high glucose (HG, 20 mM; purple, dark gray) of the human PSC-derived β cells and human islets were compared.

F: Relative gene expression levels of IGF1-binding proteins, *IGFBP3*, *IGFBP5*, and *IGFBP6* in undifferentiated PSC, DE, PP, EP, EC, and human islets are shown.

A 2-tailed paired t test analyzed differences between groups, shown as *$p < 0.05$, ****$p < 0.0001$.

4.4 Discussion

By removing Zn from cell culture media, definitive endoderm (DE) differentiation was enhanced (Figure 4.1B, D). The effect was observed only under Compl cells. While in cells pretreated with ΔMet, Zn conditions did not affect DE differentiation, suggesting its stronger effect in differentiation compared to Zn. Another finding was the variance of DE differentiation efficiency among different cell lines can be solved under a Zn-deprived medium. This is a novel procedure that helps to enhance DE differentiation in a wide range of different cell lines, as different cell lines often possess different levels of cell proliferation speed and differentiation efficiency.

Attempted to optimize Zn concentration during pancreatic differentiation, I found out that IGF1 might not be sufficient for cell survival, and instead, INS is needed. In contrast, neither IGF1 nor INS affects pancreatic β-cell differentiation. This suggested that INS signaling might be needed in part of pancreatic development for cell survival. In previously published reports regarding INS receptor and IGF1 receptor knock-out mice, normal islets or β cells were observed, suggesting INS or IGF1 receptor is not important for early β cell development (Ueki et al., 2006). Besides, their data provide genetic evidence that INS acts as a dominant role in comparison to IGF1 in promoting growth during early development. This might be the reason why in my current differentiation system, IGF1 was insufficient for cell survival. Also, as IGF1 signaling is known to be regulated through IGF1 binding proteins, I found out that several members of IGF1 binding proteins were expressed during pancreatic progenitor (PP) and endocrine cell (EC) stages (Figure 4.3F). *Insulin-like Growth Factor Binding Protein 3* (*IGFBP3*) is reported to be an inhibitor of proliferation and activation of this protein will drive cells to apoptosis (Werner et al., 2008). This might explain why IGF1 was not suitable for my culture system. Since APIDRA insulin glulisine, an insulin analog in which its Zn-binding site was mutated, is applicable to the current differentiation procedure, I still have the freedom to alter Zn concentrations during specific differentiation stages to examine the Zn effect.

Furthermore, with the combination of ΔMet and ΔZn applied to the pancreatic differentiation procedure, as high as 73.1% of INSULIN-expressing pancreatic β cells on day 33 were obtained (Figure 4.3D). Day 39 pancreatic β cells also responded to high glucose and showed glucose-stimulated insulin secretion ability at a comparable level with human islets (Figure 4.3E). This is a novel procedure for generating functional pancreatic β cells using human-induced pluripotent stem cells. As mentioned in Chapter 1.3, most of the

differentiation protocols focus on the growth factors and small molecules or the cell culture microenvironment in differentiating PSCs.

Chapter 5: Relationship between Methionine and Zinc in human pluripotent stem cells

5.1 Knockdown of *SLC30A1* gene using small interfering RNA (siRNA)

In exploring the mechanism that potentiates cell differentiation in ΔMet pretreated cells, I focused on the upregulated *SLC30A1* gene observed specifically under ΔMet pretreated conditions. This led me to alter the Zn concentrations in cell culture and demonstrate that decreased intracellular Zn contents reduced cell proliferation and increased differentiation marker expressions. However, I was not sure whether ZNT1 was involved directly in this. Therefore, a *SLC30A1* knockdown experiment was performed to investigate whether this is this target gene involved in Met metabolism, which regulates cell differentiation.

By using commercially available siRNAs, PSCs were treated with non-silencing (NS) and *SLC30A1* siRNA for 24 hours. The siRNA-treated cells were then cultured in Compl and ΔMet medium for 5 hours. The cells were collected and subjected to real-time PCR analysis and western blot (Figure 5.1A). I then examine the protein level of ZNT1 of NS and *SLC30A1* siRNA-treated PSCs. ZNT1 was detected at the protein level by western blot (Figure 5.1B). ZNT1 protein level decreased in conditions treated with *SLC30A1* siRNA. An increase of 1.4-fold of ZNT1 protein in ΔMet cells compared to Control was observed under NS siRNA conditions, suggesting the effect of ΔMet.

Given that the *SLC30A1* knockdown was successful, I then examined the gene expression of the samples. First, the results showed that *SLC30A1* was significantly downregulated compared to non-silencing control, similar results were obtained in western blotting. Gene upregulation was also not seen under ΔMet pretreated condition. Furthermore, ΔMet-responsive gene, *EGR1*, and *DHRS2* exhibited upregulation after ΔMet pretreatment, however, under both knockdown conditions. Differentiated marker genes, *GATA4,* were significantly upregulated after ΔMet treatment but did not show any difference among knockdown conditions. *PAX6* and *PECAM1* were upregulated after methionine treatment under NS siRNA conditions and did show any changes in *SLC30A1* siRNA treated conditions (Figure 5.1C).

Although *SLC30A1* led me to focus on Zn contents in PSCs and in cell culture, which regulates cell pluripotency and differentiation like ΔMet, this gene might not be the key component that causes a decrease in protein-bound Zn contents in methionine deprivation pretreatment iPS cells.

Figure 5.1

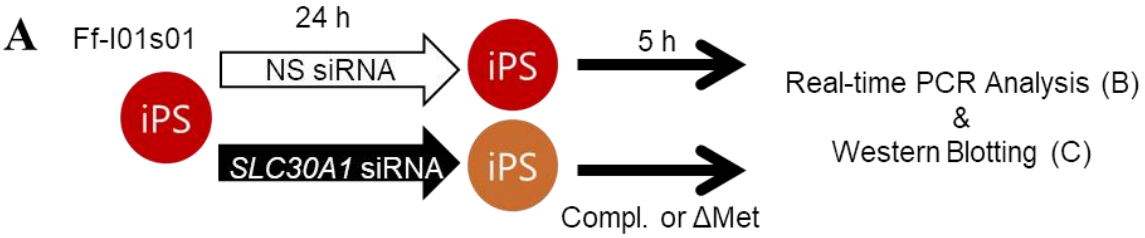
A
Ff-I01s01
24 h
NS siRNA
iPS
iPS
5 h
Real-time PCR Analysis (B)
&
Western Blotting (C)
SLC30A1 siRNA
iPS
Compl. or ΔMet

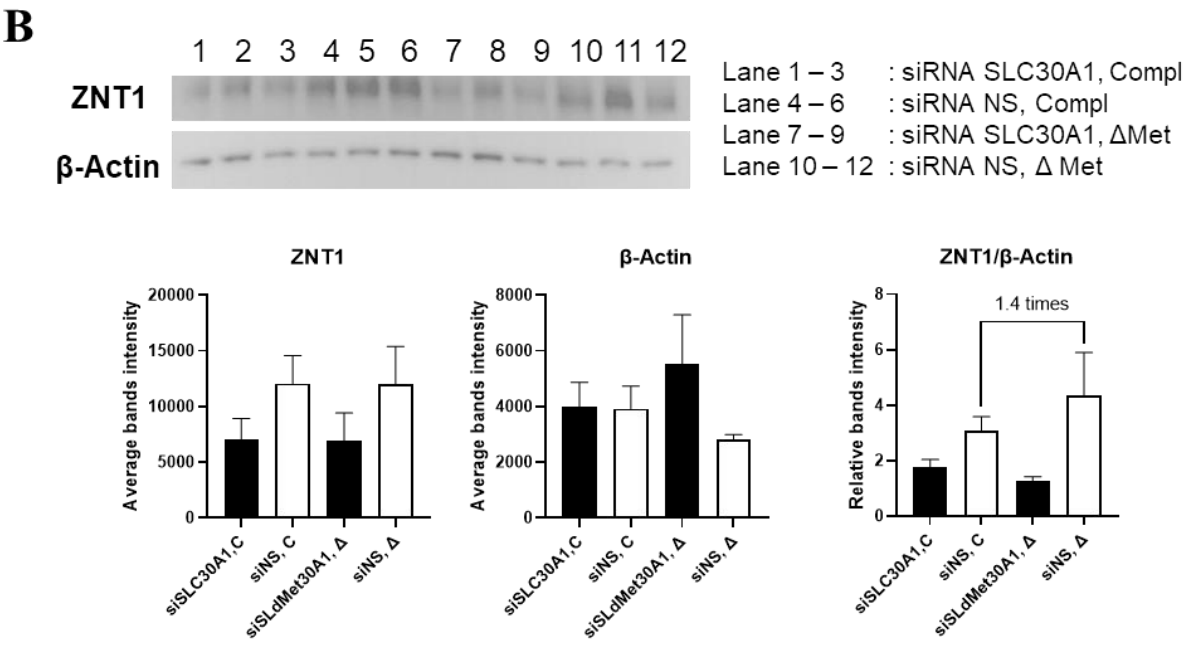
B
1 2 3 4 5 6 7 8 9 10 11 12
ZNT1
β-Actin
Lane 1 – 3 : siRNA SLC30A1, Compl
Lane 4 – 6 : siRNA NS, Compl
Lane 7 – 9 : siRNA SLC30A1, ΔMet
Lane 10 – 12 : siRNA NS, Δ Met
ZNT1
Average bands intensity
20000
15000
10000
5000
0
siSLC30A1,C
siNS, C
siSLdMet30A1, Δ
siNS, Δ
β-Actin
Average bands intensity
8000
6000
4000
2000
0
siSLC30A1,C
siNS, C
siSLdMet30A1, Δ
siNS, Δ
ZNT1/β-Actin
Relative bands intensity
1.4 times
8
6
4
2
0
siSLC30A1,C
siNS, C
siSLdMet30A1, Δ
siNS, Δ

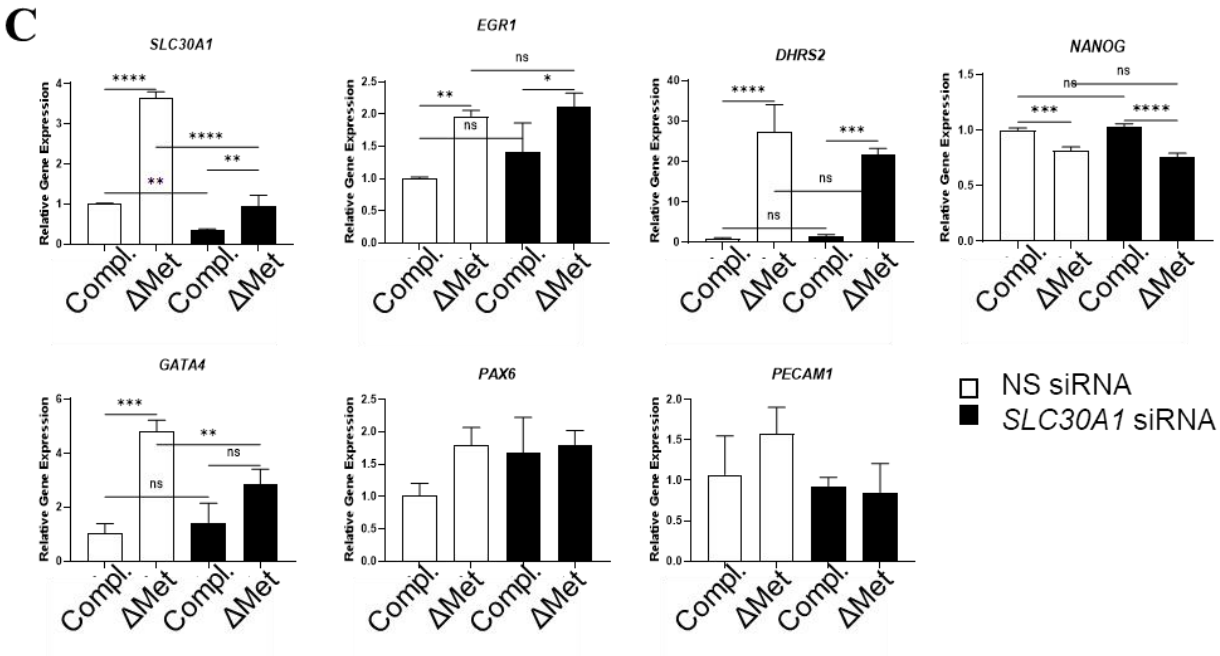
C
SLC30A1
EGR1
DHRS2
NANOG
GATA4
PAX6
PECAM1
Relative Gene Expression
Compl.
ΔMet
NS siRNA
SLC30A1 siRNA

Figure 5.1

A: A schematic diagram showing the procedure of siRNA experiments and cells were sampled for western blotting (B) and real-time PCR analysis (C).

B: Western blotting of ZNT1 and beta-Actin are shown. ZNT1 antibody was a gift from Associate Professor Kambe (Kyoto University). (Upper part) Quantification analyses of blotting bands are shown. (Lower part)

C: Relative gene expression results of *SLC30A1*, *EGR1*, *DHRS2*, *NANOG*, *GATA4*, *PAX6*, and *PECAM1* of cells treated with NS, *SLC30A1* siRNA and five hours of Compl and ΔMet conditions are shown.

Data are expressed as mean ± SEM. N=3. Differences are shown as *<0.05, **p<0.01, ***p<0.005, ****p<0.001; analyzed by a two-tailed unpaired Student's t-test.

5.2 RNA sequencing data of undifferentiated PSCs cultured under graded Zn conditions

Furthermore, to understand how Zn treatment affects gene expression, RNA sequencing was performed using 48 hours at various Zn conditions (0, 0.5, 3, 10 μM) treated PSCs (Figure 5.2A). Gene ontology (GO) enrichment analysis of the upregulated or downregulated genes was performed. Here are the top 10 gene categories that were upregulated dependently to Zn concentration, including cellular zinc ion homeostasis, mitochondrial translation elongation and termination, detoxification of copper ion, mitochondrial large ribosomal subunit, negative regulation of growth, embryonic digestive tract development, cellular response to zinc ion, copper ion and cadmium ion (Figure 5.2B, left). The upregulated genes mostly consist of the metallothionein family (MT), including *MT1E*, *MT1G*, *MT1H*, etc., were Zn-binding proteins which actively involved in various Zn activities, and mitochondrial ribosomal proteins, *MRPL16*, *39*, and *40* also involved in Zn homeostasis in cells. The top 10 gene categories that were downregulated when cells were cultured in higher Zinc concentrations include regulation of autophagy, cellular response to starvation and drugs, protein processing, etc. (Figure 5.2B, right). Overall, these genes work to adjust the Zn homeostasis in the cell environment in regulating cell growth and cell response.

Then, to examine the relationship between Met and Zn, Zn-dependent genes were compared with methionine-related genes in PSCs. These genes shown here were positively or negatively correlated in response to high Zn concentration. Genes upregulated by ΔMet, and high Zn concentration involves *EGR1*, *MT1H*, *PIM1*, *SLC30A1*, and *TNFRSF12A* (Figure 5.2C). Upregulated genes are from the MT family, which might be essential to regulate Zn for the maintenance of cell growth and function. In contrast, some of the commonly downregulated genes were shown on the left, including *GDF3,* which belongs to the TGF beta superfamily, and *SLC39A6,* which encodes a zinc influx transporter (Figure 5.2D).

Genes expressed in the methionine and cysteine cycle were also examined. Upregulation of *DNMT3B* and downregulation of *methionine adenosyltransferase 2A* (*MAT2A*) was observed when cells were cultured will higher Zn concentration (Data not shown). However, these gene changes were not reproducible when I compared them with several experiments. Further considerations of other methods might be needed to relate Zn with methionine metabolism.

Figure 5.2

A

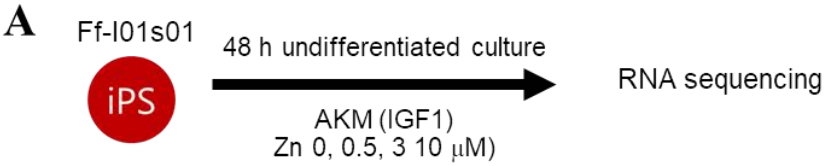

B

Category	P-value
cellular zinc ion homeostasis	2.73E-08
mitochondrial translational elongation	1.70E-07
mitochondrial translational termination	1.85E-07
detoxification of copper ion	3.19E-07
mitochondrial large ribosomal subunit	8.59E-07
negative regulation of growth	8.98E-07
cellular response to zinc ion	2.10E-06
embryonic digestive tract development	3.05E-06
cellular response to copper ion	8.02E-06
cellular response to cadmium ion	3.50E-05

Category	P-value
regulation of autophagy	5.98E-11
actin filament	3.86E-09
synapse assembly	1.20E-08
cellular response to starvation	3.45E-08
regulation of neuron projection development	2.48E-07
circadian rhythm	3.12E-07
protein processing	5.68E-07
atpase-coupled intramembrane lipid transporter activity	1.09E-06
response to endoplasmic reticulum stress	1.80E-06
cellular response to drug	2.03E-06

C

Genes upregulated by ΔMet and cytosolic Zn

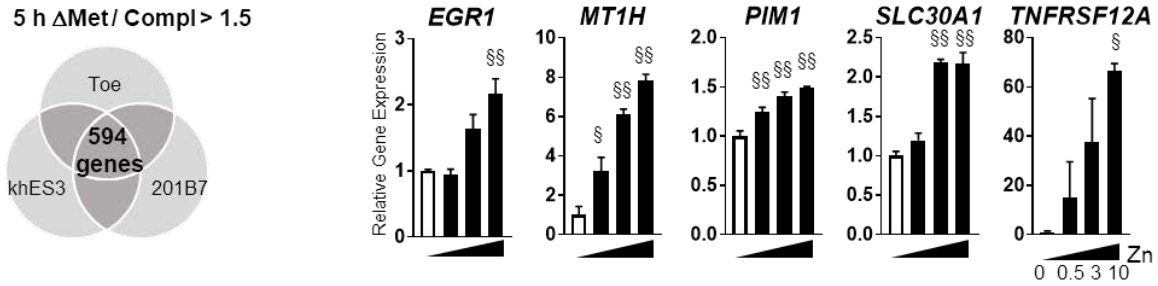

D

Genes downregulated by ΔMet and cytosolic Zn

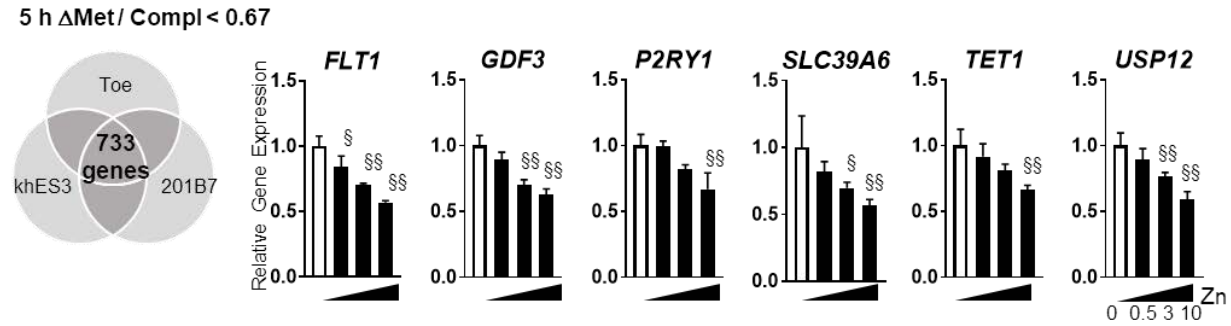

Figure 5.2

A: Schematic drawing of the PSCs culture conditions for RNA sequencing.

B: The top ten categories extracted from gene ontology (GO) enrichment analysis, for upregulated (left) or downregulated (right) genes by increasing Zn concentration.

C, D: The representative gene expression profiles, depending on the Zn concentration in the culture medium, are shown.

C: Of the 594 genes commonly upregulated >1.5-fold by ΔMet in at least two different array sets, seven genes, including *EGR1*, *MT1H*, *PIM1*, *SLC30A1*, and *TNFRF12A*, showed a significantly high coefficient of determination $|R^2| > 0.70$ with Zn.

D: Of the 733 genes commonly downregulated < 0.67-fold by ΔMet in at least two different array sets, 38 genes, including *FLT1*, *GDF3*, *P2RY1*, *SLC39A6*, *TET1*, and *USP12*, were negatively correlated in response to Zn (coefficient of determination $|R^2| > 0.70$).

Data are expressed as means ± SDs. N = 3 (biological replicates). Differences between groups were analyzed by 1-way ANOVA Dunnett's multiple comparison tests, and significant differences are shown as $^{\S}p < 0.05$, $^{\S\S}p < 0.01$.

5.3 Methionine metabolism in undifferentiated PSCs cultured under graded Zn conditions

A rapid decrease in intracellular S-adenosyl-methionine (SAM) and Met levels was observed in PSCs after ΔMet pretreatment. Also, upregulation of *MAT2A* and downregulation of *DNMT3B* are confirmed in ΔMet pretreated cells. As Zn mimics the effects of Met, I tried to measure the metabolites in ΔZn cells and examine the metabolic changes in methionine metabolism.

Undifferentiated PSCs were cultured under graded Zn concentrations (0, 0.5, 3, 10 μM) for 48 hours and sampled for real-time PCR (qPCR) analysis and metabolite measurements (Figure 5.1A). Matching the qPCR results obtained in Chapter 3.2 (Figure 3H, I), cell renewal genes, *GRB7* and *HCK* were downregulated among 0 μM Zn condition (Figure 5.3B). Differentiation genes, *GATA4*, *PAX6,* and *PECAM1* were upregulated in 0 μM Zn compared to higher Zn conditions (Figure 5.3C). This is to make sure Zn affects on undifferentiated cells. Cell morphology was also observed every day when cell culture was performed.

Then, the day 2 hPSC pellets were prepared and sent to Miura laboratory (Tokyo University) for metabolites measurement. The results were summarized in Figure 5.3DE, showing the intracellular (Figure 5.3D) and extracellular (Figure 5.3E) contents of metabolic measurements in the methionine cycle. In cells, unlike the ΔMet condition, decrease of intracellular SAM ($[SAM]_i$) level was not observed between 0 μM Zn and 3 μM Zn. $[Adenosine]_i$ significantly decreased at 0 μM Zn compared to 3 μM Zn. On the other hand, in the medium, the $[SAM]_e$, methyl-thio-adenosine ($[MTA]_e$), tetrahydrofolate ($[THF]_e$), $[SAH]_e$, $[Glycine]_e$ levels significantly changed between 0 μM Zn and 3 μM Zn. Since the culture medium contains methionine and other amino acids that cells consume accompanying cell growth, the raw values were subtracted from the initial amounts of the metabolites existing in the fresh medium and normalized the values to 24 hours and the cell number. A minus value represents the consumption by the cells, and a plus value represents the excretion from the cells (nmol / 24h /1x10^6 cells). Excess excretions of SAM, SAH, and MTA were observed at 0 μM Zn, compared to 3 μM Zn. As SAM, SAH and MTA are the main components in the methionine cycle. The results suggested that Zn deprivation affects Met metabolism.

Figure 5.3

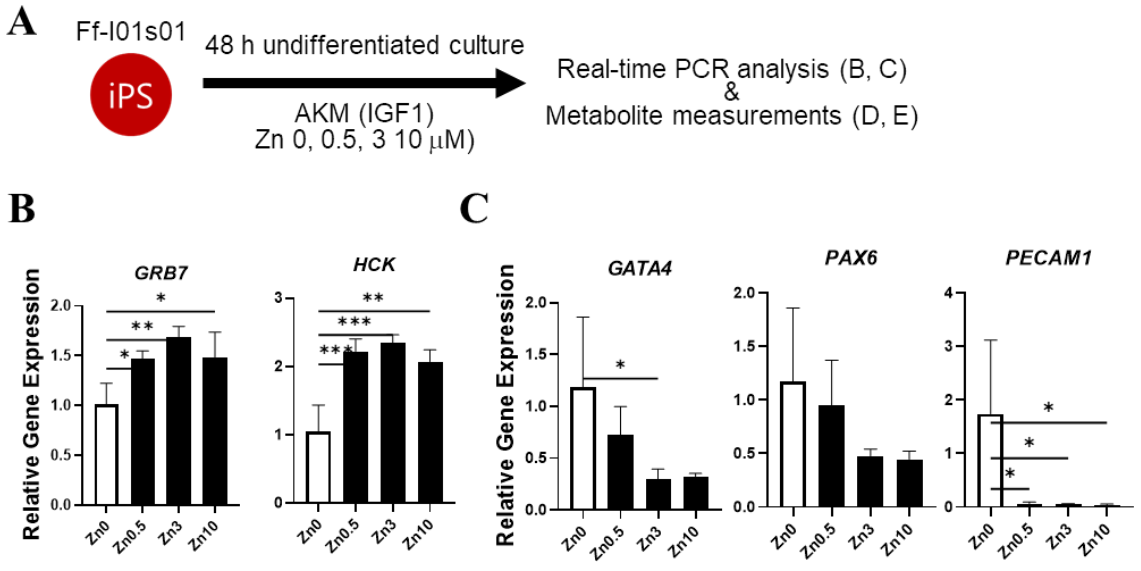

Figure 5.3

A: A schematic diagram of the PSCs culture conditions for real-time PCR analysis (B, C) and intracellular Met, SAM, and SAH metabolites measurements.

B: Relative gene expression results of cell renewal marker, *GRB7* and *HCK* are shown.

C: Relative gene expression results of differentiation marker, *GATA4*, *PAX6*, and *PECAM1* are shown.

Data are expressed as mean ± SEM. N=3. Differences are shown as *<0.05, **p<0.01, ***p<0.005; analyzed by a two-tailed unpaired Student's t-test.

Figure 5.3

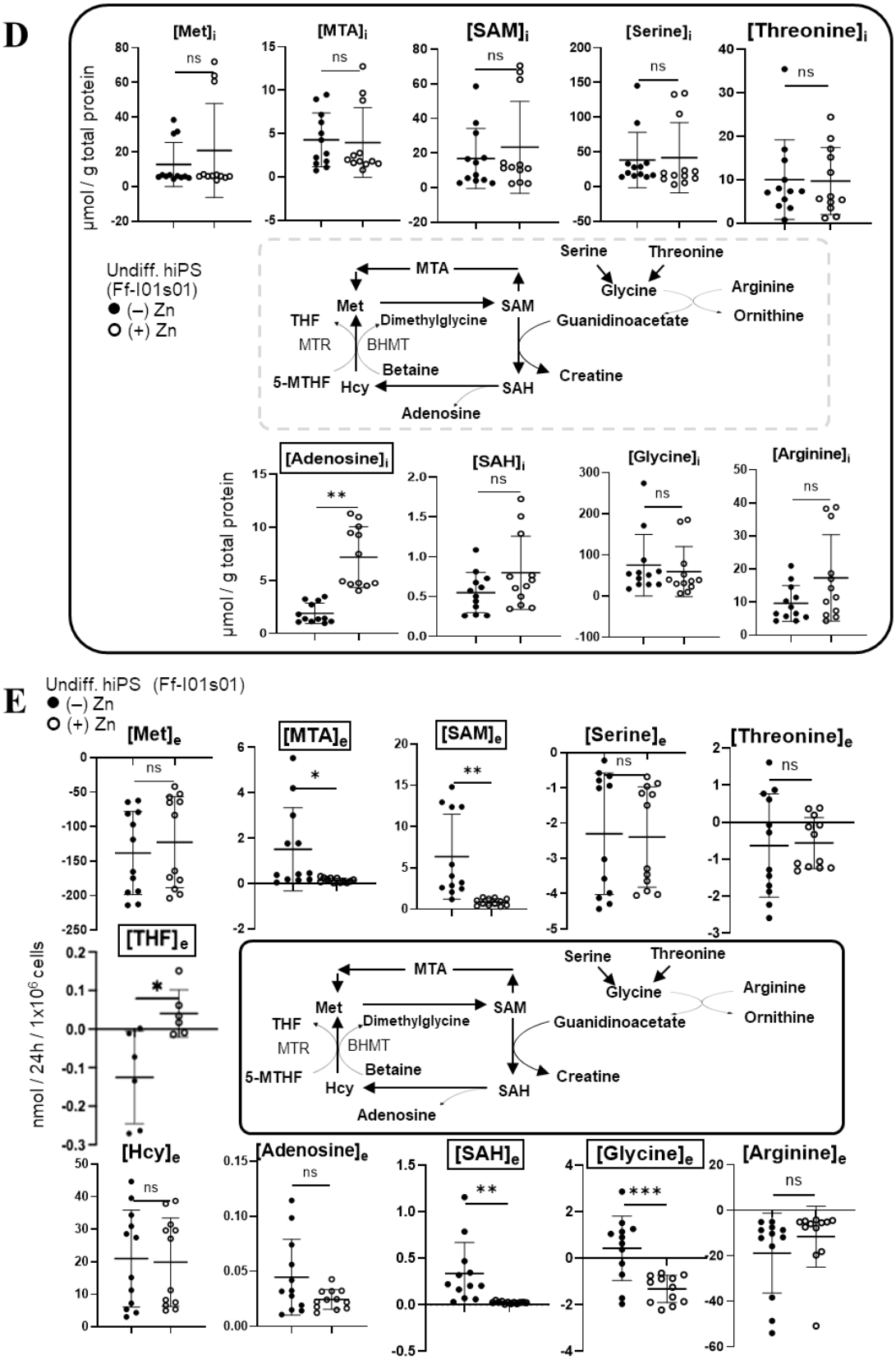

Figure 5.3

D and E: Intracellular (D) and extracellular (E) contents of methionine cycle metabolites measurement at 0 µM Zn (closed circle (-) Zn) or 3 µM Zn (open circle (+) Zn).

5.4 Discussion

After knowing that ΔZn mimics the effects of ΔMet pretreatment, I am curious about the relationship between them in regulating the maintenance of PSCs and cell differentiation. Therefore, I first focused on the *SLC30A1* gene that leads me to Zn. *SLC30A1* gene was successfully knocked down by siRNA treatment. The knockdown was also confirmed through western blotting. However, gene expression levels in ΔMet-responsive genes, *EGR1* and *DHRS1* were not affected by *SLC30A1* knockdown. Also, in knockdown cells, differentiation marker genes *GATA4*, *PAX6*, and *PECAM1* were not downregulated. This suggested that *SLC30A1* might not be the key component that interacts with ΔMet-responsive genes and differentiation genes. I think that *SLC30A1* might not act as the regulator to drive the release of Zn from Zn-binding protein (Figure 2.2F). Recently, it is reported that the expression of ZNT1 would increase depending on the increase of labile Zn ions in cells (Nishito and Kambe, 2019). Therefore, I suspect that ZNT1 might be just a Zn sensor in PSCs. However, to further confirm this matter, inducible knockdown using a short hairpin RNA (shRNA) can be performed to obtain better knockdown efficiency for further consideration.

From the RNA sequencing results, metallothionine (MT) family members and several members of the *MRPL* gene family are the top genes that are upregulated by Zn concentration in PSCs. As mentioned in Chapter 1, MT participates in uptake, transport, and regulation of Zn in the human body. This explains the expression of these MTs might be essential to maintain Zn homeostasis at a proper range in cells for the maintenance of cell growth and function. Mitochondrial ribosomal proteins are reported to function as Zn storage (Danchin, 2020). These confirmed that the upregulation of MT and *MRPL* genes are resulted from increasing Zn concentrations in cells.

The link between Met and Zn was determined when I attempted to compare Zn-dependent gens and Met-related genes in PSCs. First, I found significant upregulation of *DNMT3B* and downregulation of *MAT2A* in cell group cultured with high Zn (10 μM) concentration. However, this result was not reproducible when similar experiments were repeated. Therefore, I also considered measuring intracellular metabolites involved in the Met cycle (Figure 5.3D, E). In our previous report (Shiraki et al., 2014), significantly decreased $[SAM]_i$ levels were confirmed in ΔMet cells. However, the decrease of SAM was not confirmed in 0 μM Zn cells. Under 0 μM Zn condition, $[Adenosine]_i$ significantly decreased. It is reported that in rats and cell culture models, zinc deficiency impairs the activities of major ectoenzymes and strongly suppresses adenine-nucleotide hydrolysis

(Takeda et al., 2018). Adenine-nucleotide hydrolysis is mediated by a Zn-dependent ALP, whose activity is downregulated upon Zn deprival (Figure 5.3F). Therefore, the decreased $[Adenosine]_i$ explained the decreased adenine-nucleotide metabolism under Zn deficiency.

It is known that betaine homocysteine S-methyltransferase (BHMT) and 5-methyl-tetrahydrofolate-homocysteine methyltransferase (MTR) in methionine cycle (Figure 5.3DE) are Zn-dependent enzymes. BHMT and MTR catalyze the conversion of HCY to methionine and require Zn for their catalytic activities (Evans et al., 2002; González et al., 2004; Koutmos et al., 2008). Depletion of Zn might slow down the converting process, which then affects the methionine metabolism. From the metabolite measurement, the significant reduction of $[THF]_e$ at 0 μM Zn indicated the inhibition of MTR, which led to the inhibition of HCY conversion to Met. Also, the reduction of $[Adenosine]_i$ under 0 μM Zn condition indicated the inhibition of SAH conversion to HCY. Unlike the previous results seen in ΔMet cells, the HCY excretion was not inhibited in 0 μM Zn cells. This suggested that an accumulation of HCY occurred under 0 μM, in other words, it triggered a 'traffic jam' (a decreased flow) of the methionine metabolism. HCY is a toxic metabolite; cells sense HCY accumulation and excrete the HCY. The $[HCY]_e$ is ~1/8-fold of the methionine consumed and ~ 4-fold of $[SAM]_e$. Taken together, the measurement results suggest that Zn and Met metabolisms are interdependent.

Figure 5.3

F

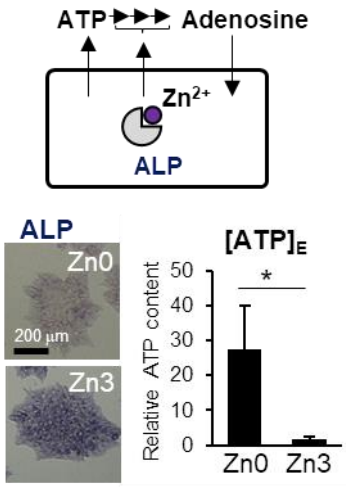

Figure 5.3

F: Cell were analyzed for alkaline phosphatase (ALP) staining (lower left) and extracellular ATP contents (lower right). Scale bar: 200 μm.

Chapter 6: Conclusion

6.1 Conclusion

In this paper, I first aimed to seek the key factor that leads to differentiation potency in methionine deprivation (ΔMet) pretreated undifferentiated pluripotent stem cells (PSCs). Then I found the upregulation of *SLC30A1*, a gene that encodes a zinc (Zn) exporter, specifically in ΔMet cells. Also, protein-bound Zn content is decreased in ΔMet cells. These results brought me to focus on Zn, an essential trace metal in the human body. Zn in cells is also known as signaling ions for intra- and intercellular communications. Therefore, I introduced a custom-made culture media, Zn deprived (ΔZn) media, to investigate the effect of Zn in undifferentiated PSCs and in pancreatic differentiation.

As a result, I found that Zn supports PSCs' growth. Zn addition reduced definitive endoderm (DE) differentiation and impacted pancreatic differentiation. Zn and insulin supplements are both needed for the later stages of pancreatic differentiation. In short, I found that Zn and Met share similar effects in regulating the maintenance and differentiation of PSCs. Furthermore, I tried to determine the relationship between Zn and Met. Comparing the gene expression profile between PSCs treated with increasing Zn concentration and those treated with ΔMet, common gene expression was found upon the changes in Zn and Met. Also, the relationship between Met and Zn was confirmed by analyzing intracellular Met-cycle metabolites in cells cultured at different Zn concentrations. SAM, and SAH excretions were observed under ΔZn cell culture conditions but not in control. These results suggested that PSCs cultured under the ΔZn condition altered Met metabolism. My study results showed a link between Met metabolism and Zn signaling (Figure 6).

Overall, my research revealed the roles of Zn in the maintenance of undifferentiated PSCs and in pancreatic differentiation. The importance of Zn in maintaining pluripotency and in pancreatic β cells has been reported (Chimienti et al., 2005; Pfaender et al., 2016; Rutter and Chimienti, 2015). However, the effect of Zn during pancreatic differentiation of PSCs is a new focus in the research field. The study is meaningful in understanding the role of Zn during pancreatic development.

Figure 6

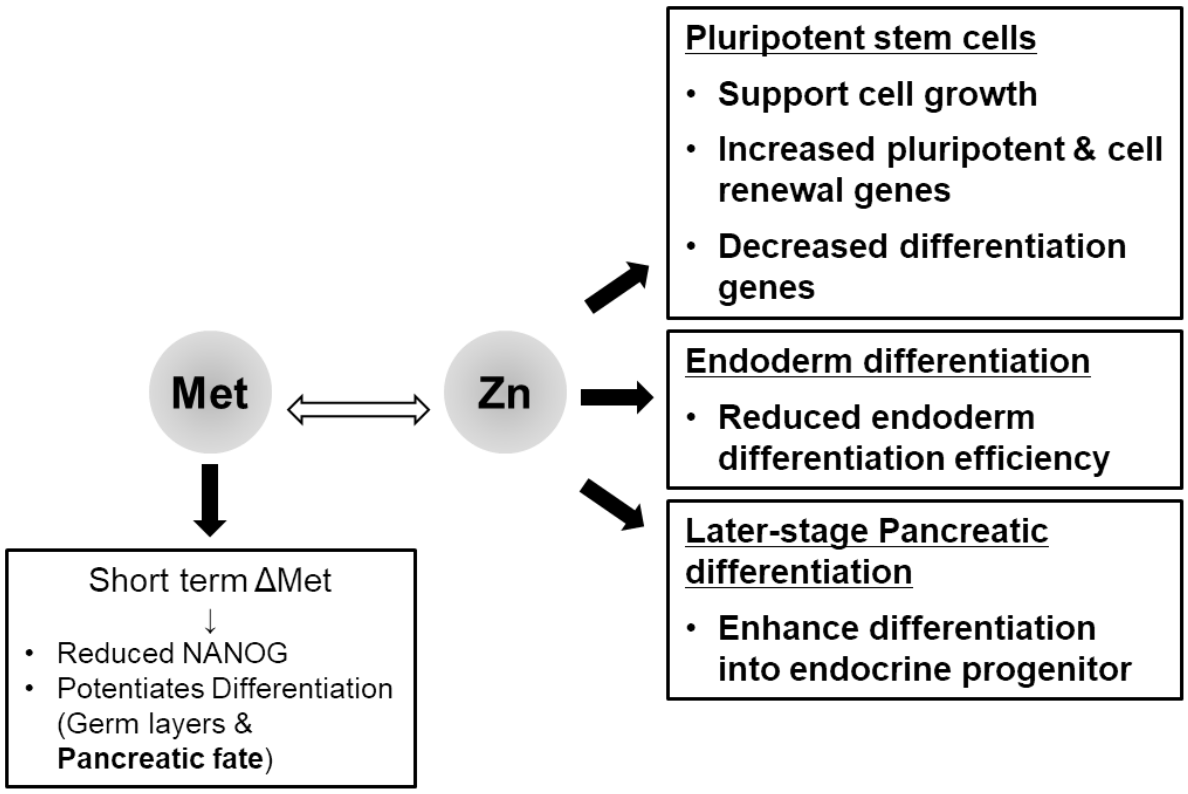

Figure 6A: A schematic diagram showing a summary of this study. Bold words represent the overall results obtained. A link was found between Zn and Met in regulating the maintenance and differentiation of PSCs.

6.2 Future perspectives

The general goal of the Kume & Shiraki Lab is to generate functional human PSC-derived pancreatic β cells as a cell source for pancreas or islet transplantation. My optimized pancreatic differentiation procedures have proven that functional pancreatic β cells incomparable with human islets can be generated. A further research objective will include testing the *in vivo* functionality of PSC-derived pancreatic β cells. Also, the maintenance culture of pancreatic β cells should be studied too. It is because the ability of insulin-secreting PSC-derived pancreatic β cells will deteriorate during the long term of culture. A culture medium that can maintain the viability of pancreatic β cells and the hormone secretion ability would be helpful in solving this issue. Last would be the large-scale cultivation of pancreatic β cells. The current cell culture is enough to perform transplantation into mice to check the in vivo functionality of PSC-derived pancreatic β cells. However, it is not enough when it comes to human transplantation. At least 100 times more cells are needed to achieve transplantation into humans. Therefore, performing large-scale culture of pancreatic β cells is needed to achieve sufficient cell amount to be used as regenerative medicine.

Next, although the decrease in intracellular protein-bound Zn was shown to be caused by a temporal increase of HCY, the exact molecular mechanism is still unknown. A further objective could be to identify the metal-binding site to track down the specific protein. There were methods reported in identifying novel Zn-binding proteins that can be used as reference (Furukawa et al., 2018; Jabrani et al., 2017).

Methods

Cell line

Toe human iPS cell (hiPSC) line was established by Toyoda M., Kiyokawa N., Okita H., Miyagawa Y., Akutsu H. and Umezawa A. in National Institute for Child Health and Development, Tokyo. RPChiPS771 human iPSCs were obtained from REPROCELL Inc. (Tokyo). This cell line is which was established using a synthetic self-replicative RNA (Yoshioka et al., 2013). Human ESCs, KhES3 (Suemori et al., 2006), were a gift from Dr N. Nakatsuji and Dr H. Suemori (Kyoto University, Japan). 201B7 (Takahashi and Yamanaka, 2006) and 8 others human iPS cell lines, Ff-I01s01, Ff-I14s03, Ff-I01s04, Ff-I14s04, Ff-MH09s01, Ff-MH15s01, Ff-MH15s02 and Ff-MH23s01, were obtained from the Center for iPS Cell Research and Application, Kyoto University (CiRA). These 8 cell lines originated from the iPS cell stock for regenerative medicine. They are generated by gene-integration-free iPSCs from donors whose human leukocyte antigen (HLA) type is homozygous at three major HLA loci, which will match approximately 20 percent of Japanese population.

Maintenance culture of undifferentiated human iPSCs

Cryopreserved human iPSCs were thawed and cultured on 100 mm CellBIND cell culture dish (Corning) coated with SynthemaxII (functionalized with short peptide sequences derived from the vitronectin protein, which is covalently linked to the synthetic acrylate polymer, Corning) with StemFit®AK03N, with addition of B and C solution (Ajinomoto Inc., Japan) in a 37°C incubator, 5% CO_2. The iPSCs from CiRA were cultured using AK03N while the others using StemFit®AK02N. The cells were fed every day and then passaged when reaching 80-90% confluency.

Cell passage was performed as follows. The media was removed, and the cells were washed using sterilized phosphate buffered saline (PBS). 1x TrypLE™ Select (Gibco) was then added and the cells were being incubated at 37°C for 5 minutes. After the incubation, the 1x TrypLE™ Select was removed and medium was added. Cell scrapper was used to remove the cells from the culture dish and cells were collected with the medium. The collected cells were centrifuged at 1000 rpm for 5 minutes while the number of cells collected was then calculated by using automated cell counter, Countess II FL (Thermo Fisher Scientific). Next, the cells were resuspended with AK03N media and replated with 1 x 10^6 cells per 100 mm dish. The number of cells plated is varied depends on the culture dish used. (6-well plate: 1 x 10^5 cells/well, 96-well plate: 2000 cells/well)

In vitro pancreatic differentiation of undifferentiated human iPSCs

For initiation of pancreatic differentiation, human iPSCs were dissociated with 1x TrypLE™ Select (Gibco) and seeded at a density of 5 x 10^6 cells/well on 6-well Greiner CELLSTAR® multiwell culture plate (Sigma Aldrich). They were cultured for one day using AK03N media containing 10 μM ROCK inhibitor (Y-27632; Wako) on top of an orbital shaker with 95 rpm to form cell spheroids. Then, methionine deprivation pretreatment was done by culturing the cells for 5 hours in Met-deprived StemFit KA01 (=AK03N ΔMet) medium or control complete media (StemFit KA01 + 100 μM methionine) (Ajinomoto, Tokyo), before initiation of differentiation. The media used for pancreatic differentiation basically followed that reported by our group, with minor modifications. After 5 hours complete or methionine deprivation pretreatment, initiation of differentiation was done by replacing the culture with Medium 1 (Day 0). The detailed media used are as following.

For differentiation of RPChiPS771 human iPSCs

Medium 1 (M1); day 0-2 (Without CHIR99021 on day 1-2)	Concentration	Source	Product Code
DMEM (4500 mg/L glucose)	-	Gibco	11965092
B-27 insulin (+) supplement	2%	Life Technologies	17504044
Activin A (0.1 mg/ml)	100 ng/ml	Cell Guidance Systems	GFH6
CHIR99021 (3 mM)	3 μM	Wako	034-23103
Medium 2 (M2); day 3-4	Concentration	Source	Product Code
RPMI	-	Gibco	11875093
B-27 insulin (-) supplement	2%	Life Technologies	A1895601
FGF10 (50 μg/ml)	50 ng/mL	PeproTech, Inc.	AF-100-26
SANT-1 (2.5 mM)	250 nM	Sigma	S4572-5MG

Medium 3 (M3); day 5-10	Concentration	Source	Product Code
DMEM (4500 mg/L glucose)	-	Gibco	11965092
B-27 insulin (+) supplement	1%	Life Technologies	17504044
SANT-1 (2.5 mM)	250 nM	Sigma	S4572-5MG
All-Trans Retinoic Acid (100 mM)	2 μM	Stemgent	04-0021
LDN-193189 (1 mM)	100 nM	Wako	SML0559
Medium 4 (M4); day 11-12	Concentration	Source	Product Code
DMEM (4500 mg/L glucose)	-	Gibco	11965092
B-27 insulin (+) supplement	1%	Life Technologies	17504044
LDN-193189 (1 mM)	100 nM	Wako	SML0559
TGF-β type I receptor kinase inhibitor II	5 μM	Wako	018-23023
Indolactam V (300 μM)	300 nM	R&D Systems	3651
Medium 5 (M5); day 13-25	Concentration	Source	
Knockout DMEM/F-12	-	Gibco	12660012
B-27 insulin (+) supplement	1%	Life Technologies	17504044
Nicotinamide (1 M)	10 mM	Sigma	N0636
Exendin 4 (500 μg/ml)	50 ng/ml	Cell Sciences	CRE117C
N-Acetyl-L-Cysteine (100 mM)	1 mM	Nacalai Tesque	00512-84
$ZnSO_4$ (10 mM)	10 μM	Sigma	Z0251-100G

All media (Medium 1 - 4) were supplemented with L-Glutamine, Penicillin-Streptomycin (PS; Nacalai Tesque), MEM Non-essential amino acid (NEAA; Life Technology), and 2-Mercaptoethanol (2-ME; Sigma).

For differentiation of human iPSCs from HLA homozygote donors, the media used for differentiation are as following.

AK03N media, represented by AKM (INS) was INS- and Zn-containing media. Zn-deprived basal media used was KA02 media, AKM (Zn0). AKM (IGF1) media was AKM (Zn0) medium supplemented with 100 ng/mL IGF1 (Cell Guidance Systems or Oriental Yeast Co., Ltd). AKM (INS*) medium was AKM (Zn0) medium supplemented with 19.4 ug/mL APIDRA insulin glulisine (Sanofi S.A.), an insulin analog with no hexamer-promoting Zn. The concentration of insulin glulisine in AKM (INS*) is the same as that of INS in chemically defined E8 medium (Chen and Khillan, 2010). All media used here is without addition of C solution (FGF2).

AKM (IGF1 or INS*) medium are used for experiments in Figure 4.1, 4.2, and Figure 4.3 Medium 1 and 2.

AKM (INS) is used during experiments in Figure 4.3 Medium 3 – 6.

Medium 1 (M1-AKM); day 0-2 (Without CHIR99021 on day 1-2)	Concentration	Source	Product Code
AKM (Zn0) medium (KA02)	-	Ajinomoto	
Penicillin-Streptomycin (PS) (10,000 U/mL)	1%	Nacalai Tesque	26252-94
Recombinant human IGF1 (100 mg/mL)	100 ng/mL	Cell Guidance Systems	47063900
$ZnSO_4$ (10 mM)	0, 0.5, 3 μM	Sigma	Z0251-100G
Activin A (0.1 mg/ml)	100 ng/ml	Cell Guidance Systems	GFH6
CHIR99021 (3 mM)	3 μM	Wako	034-23103

Medium 2 (M2-AKM); day 3-4	Concentration	Source	Product Code
AKM (Zn0) medium (KA02)	-	Ajinomoto	
PS (10,000 U/mL)	1%	Nacalai Tesque	26252-94
Recombinant human IGF1 (100 mg/mL)	100 ng/mL	Cell Guidance Systems	47063900
$ZnSO_4$ (10 mM)	0, 0.5 μM	Sigma	Z0251-100G
KGF (50 μg/ml)	50 ng/mL	Fujifilm-Wako	119-00661
Vitamin C (4.4 mg/mL)	44 μg/mL	Sigma	A4544

Medium 3 (M3-AKM); day 5-7	Concentration	Source	Product Code
AKM (INS/Zn3) (Figure 4.3)	-	Ajinomoto	
AKM (IGF1 or INS*) (Figure 4.2)	-	Ajinomoto	
PS (10,000 U/mL)	1%	Nacalai Tesque	26252-94
KGF (50 μg/ml)	50 ng/mL	Fujifilm-Wako	119-00661
Vitamin C (4.4 mg/mL)	44 μg/mL	Sigma	A4544
SANT-1 (2.5 mM)	250 nM	Sigma	S4572-5MG
All-Trans Retinoic Acid (100 mM)	2 μM	Stemgent	04-0021
Y27632 (10 mM)	10 μM	Fujifilm-Wako	251-00514
LDN-193189 (1 mM)	0.2 μM	Sigma	SML0559
PdBU (5 mM)	500 nM	LC laboratories	P-4833

Medium 4 (M4-AKM); day 8-12	Concentration	Source	Product Code
AKM (INS/Zn3) (Figure 4.3)	-	Ajinomoto	
AKM (IGF1 or INS*) (Figure 4.2)	-	Ajinomoto	
PS (10,000 U/mL)	1%	Nacalai Tesque	26252-94
KGF (50 μg/ml)	50 ng/mL	Fujifilm-Wako	119-00661
Vitamin C (4.4 mg/mL)	44 μg/mL	Sigma	A4544
SANT-1 (2.5 mM)	250 nM	Sigma	S4572-5MG
All-Trans Retinoic Acid (100 mM)	100 nM	Stemgent	04-0021
Y27632 (10 mM)	10 μM	Fujifilm-Wako	251-00514
Activin A (0.1 mg/ml)	5 ng/mL	Cell Guidance Systems	GFH6
Medium 5 (M5-AKM); day 13-16	Concentration	Source	Product Code
AKM (INS/Zn3) (Figure 4.3)	-	Ajinomoto	
AKM (IGF1 or INS*) (Figure 4.2)	-	Ajinomoto	
PS (10,000 U/mL)	1%	Nacalai Tesque	26252-94
Vitamin C (4.4 mg/mL)	44 μg/mL	Sigma	A4544
SANT-1 (2.5 mM)	250 nM	Sigma	S4572-5MG
All-Trans Retinoic Acid (100 mM)	100 nM	Stemgent	04-0021
Alk5 inhibitor (10 mM)	10 μM	Wako	018-23023
Betacellulin (100 μg/mL)	20 ng/mL	Pepro Tech, Inc.	100-50
L-3,3',5-Triiodotyronine (T3) (100 μM)	1 μM	Sigma	T6397-1G

LDN-193189 (1 mM)	0.2 μM	Sigma	SML0559
Heparin (1 mg/mL)	10 μg/mL	Sigma	H3149-50KU
Gamma secretase XX inhibitor (10 mM)	1 μM	Sigma	565790-1MGCN
Medium 5 (M5-AKM); day 17-20	Concentration	Source	Product Code
AKM (INS/Zn3) (Figure 4.3)	-	Ajinomoto	
AKM (IGF1 or INS*) (Figure 4.2)	-	Ajinomoto	
PS (10,000 U/mL)	1%	Nacalai Tesque	26252-94
All-Trans Retinoic Acid (100 mM)	25 nM	Stemgent	04-0021
Alk5 inhibitor (10 mM)	10 μM	Wako	018-23023
Betacellulin (100 μg/mL)	20 ng/mL	Pepro Tech, Inc.	100-50
L-3,3',5-Triiodotyronine (T3) (100 μM)	1 μM	Sigma	T6397-1G
Gamma secretase XX inhibitor (10 mM)	1 μM	Sigma	565790-1MGCN
Medium 6 (M6-AKM); day 21 onwards	Concentration	Source	Product Code
AKM (INS/Zn3) (Figure 4.3)	-	Ajinomoto	
PS (10,000 U/mL)	1%	Nacalai Tesque	26252-94
$ZnSO_4$ (10 mM)	10 μM	Sigma	Z0251-100G

Human islets

Non-diabetic human islets were obtained from Prodo Laboratories (HP17040-01, HP-18157-01, and HP-20003-01), cultured in Prodo Islet Medium (Prodo Laboratories), and used for glucose-stimulated insulin secretion analysis (Figure 2.1C & 4.3E).

Zn deprivation from the medium using Chelex 100

Chelex 100 resin was prewashed following manufacturer's instructions (BioRad Laboratories). The schematic diagram below showed the detailed procedure. Human iPSCs maintenance media 40 mL added with prewashed Chelex 100 resin 1.2 g were incubated for 2 hour 45 minutes with rotation, filtered (0.22 μm) and quantified for the contents of metals by Ajinomoto Inc. Control complete media was made by adding back all heavy metals, $ZnSO_4$ $7H_2O$ (Sigma), Fe $(NO_3)_3$ $9H_2O$ (Wako, Tokyo), $CaCl_2$ (Nacalai Tesque, Kyoto), $MgSO_4$ (Sigma). Zn was excluded to make Zn deprived medium.

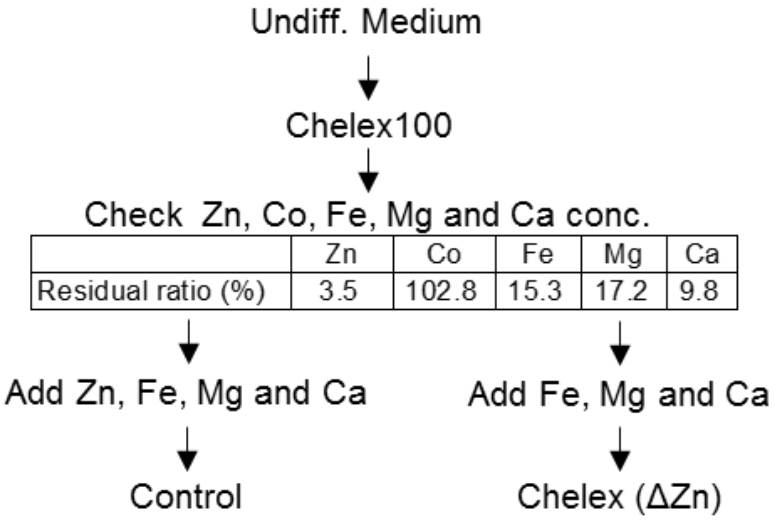

	Zn	Co	Fe	Mg	Ca
Residual ratio (%)	3.5	102.8	15.3	17.2	9.8

201B7 undifferentiated hiPSCs were dissociated and plated at $1x10^5$ cells /well on SynthemaxII coated plates 6-well plates (Corning) and cultured 37°C for 24 hours. The cells were then washed with PBS (-) and with the medium replaced with Zn deprived or control complete medium described above, and cultured for 24 hours, 48 hours or 72 hours, then the cells were dissociated, cell counted and harvested.

Zn and heavy metal content analysis

Intracellular free and protein bound heavy metal (Zn, Co, Fe, Mg, Ca) contents were measured using High Performance Liquid Chromatography (HPLC) coupled to ICP-MS (Inductively Coupled Plasma -Mass Spectrometry) (HPLC-ICP-MS) in Ajinomoto Inc. as previously described (Arakawa et al., 2016). Contents of heavy metals in the medium were measured before and after Chelex 100 treatment, then added back (except Zn for making ΔZn medium).

HCY treatment of cell lysates from hiPSCs

201B7 iPSCs cultured for 5 hours in complete medium or ΔMet medium were harvested, and cell lysates were prepared as described (Arakawa et al., 2016). The lysates were added with HCY at 1, 5, 10, 50, 500, 1000, or 2000 μM and incubated for 2 hours at 4°C. The contents of protein-bound metal (Zn, Cu, Fe) were then measured using the method described above.

Real time RT-PCR analysis

RNA was extracted from iPSCs using the RNeasy mini-kit, or All prep (DNA/RNA) Mini Kit (Qiagen, Germany) and then treated with DNase (Qiagen), or Cica geneusR RNA Prep Kit (For Tissue) (Kanto Chemical, Japan). For reverse transcription reactions, 1 μg RNA was reverse transcribed using PrimeScript™ RT Master Mix (Takara, Japan). For real-time PCR analysis, the mRNA expression was quantified with TB Green Premix Ex Taq II on a StepOne Plus (Applied Biosystems, Foster City, CA). The PCR conditions were as follows: Initial denaturation at 95°C for 30 seconds, followed with denaturation at 95°C for 5 seconds, annealing and extension at 60°C for 30 seconds, for up to 40 cycles. Target mRNA levels were expressed as arbitrary units and were determined using the ΔΔcT method.

Immunocytochemistry

In each stage of the cell culture, a portion of the cells were dissociated and replated on 96-well plate. The cells were cultured in 37°C incubator overnight. On the next day, the cells were fixed in 4% paraformaldehyde (PFA) in phosphate buffered saline (PBS) for 1 hour at room temperature. After removal of PFA solution, the fixed cell was rinsed three times with 0.1% Tween 20 (Nacalai Tesque) / PBS (PBS-T) and then permeabilized with 1% Triton-100 (Nacalai Tesque) for 15 minutes. The permeabilized cells were rinsed one time with PBS-T and were then incubated with 20% Blocking One (Nacalai Tesque) / PBS-T for blocking. After blocking, the cells were incubated with the diluted antibody in 20% Blocking One / PBS-T overnight at 4°C. After washing the cells in PBS-T, cells were incubated with the secondary antibody and 6-diamidino-2-phenylindole (DAPI) (Roche Diagnostics) in 20% Blocking One / PBS-T for 2 hours at room temperature in the dark. Images were captured using an ImageXpress Micro scanning system (Molecular Devices, Japan), and quantitative analysis was performed using the MetaXpress cellular image analysis software (Molecular Devices). The details of primary and secondary antibodies used are shown below.

For whole mount immunostaining of spheroids, 10 – 30 spheroids were collected and fixed in 4% PFA for 1 hour at room temperature. After removal of PFA solution, the fixed spheroids are rinsed with PBS-T and then permeabilized with 1% Triton-100 for 30 minutes. Spheroids were rinsed up to four times with PBS-T and were then incubated with 20% Blocking One / PBS-T for blocking, followed by primary and secondary antibody incubation procedure described above.

Primary Antibody	Source	Product Code	Dilution
Goat anti-SOX17	R&D Systems, Inc.	AF1924	1:100
Mouse anti-OCT3/4	Santa Cruz Biotechnology, Inc.	sc-5279	1:100
Goat anti-PDX1	R&D Systems, Inc.	AF2419	1:100
Rabbit anti-SOX9	Merck Millipore	AB5535	1:300
Mouse anti-NKX6.1	Developmental Studies Hybridoma Bank	F55A1-c	1:100
Guinea Pig anti-INSULIN	DakoCytomation Japan	A0562	1:1000
Secondary Antibody	**Source**	**Product Code**	**Dilution**
Alexa 568 donkey anti-goat IgG	Invitrogen	A11057	1:1000
Alexa 488 donkey anti-mouse IgG	Jackson ImmunoResearch Inc.	715-546-150	1:1000
Alexa 488 donkey anti-guinea pig IgG	Jackson ImmunoResearch Inc.	115-605-164	1:1000
Alexa 647 donkey anti-mouse IgG	Jackson ImmunoResearch Inc.	706-546-148	1:1000
Alexa 647 donkey anti-rabbit IgG	Jackson ImmunoResearch Inc.	711-606-152	1:1000

Glucose Stimulated Insulin Secretion Assay

For RPChiPS771 PSC-derived pancreatic differentiated cells

Differentiated cells at the end of stage 5 were washed three times and then pre-incubated at 37°C for 30 minutes with DMEM (Life Technologies) containing minimal essential medium, 0.2% bovine serum albumin and 2.5 mM glucose at 600 μL per well in 24-well plate. Cells were inserted into Transwell (Corning #3415) then incubated at 37°C for 1 hour with DMEM containing 2.5 mM glucose at 600 μL per well. The culture medium was collected (Low glucose), and the same cells were further incubated with DMEM containing 20 mM glucose, 600 μL per well at 37°C for another 1 hour. The culture media were collected (High glucose) and stored at -80°C until analysis. Next, the cells were lysed with RLT plus buffer (Qiagen). C-peptide secretion into the culture media were measured using the human C-peptide ELISA Kit (ALPCO Diagnostics). The amount of C-peptide was normalized to the amount of the total DNA concentration in the corresponding cell lysate. DNA were extracted using All prep (DNA/RNA) Mini Kit (Qiagen).

For Ff-I01s01 PSC-derived pancreatic differentiated cells

Differentiated cells were loaded on Transwell (Corning #3415) and pre-incubated for 4 times 10 minutes and another 30 minutes at 37°C in low glucose (2.5 mM ~ 3.0 mM) HKRB buffer (HEPES Krebs-Ringer Bicarbonate buffer, Cosmo Bio) with 0.2% BSA, on an orbital shaker (70 rpm). The buffer was collected (Low glucose), and cells were further incubated in high glucose (20 mM) HKRB buffer with 0.2% BSA, at 37 °C on an orbital shaker (70 rpm) for another 1 hour. The collected culture supernatant (High glucose) was stored at -30 °C until analysis. Cells were lysed, RNA and DNA were purified using AllPrep DNA/RNA Micro Kit (Qiagen). C-peptide secretion was measured using a human C-peptide ELISA Kit (Mercodia). The amount of C-peptide was normalized to the amount of total DNA contents in the corresponding cell lysate.

Measurement of Cell Proliferation (EdU incorporation)

The incorporation of EdU into genomic DNA during the S phase of the cell cycle to measure cell proliferation. Cells were incubated with EdU/medium for 30 minutes after cultured in various Zn condition. Then the cells were fixed, permeabilized and ready for EdU detection. The cells were incubated with reaction cocktail (100 mM Tris-HCl pH8.0, 4 mM $CuSO_4$, 50 mM Ascorbic acid, 488 Alexa Fluor Azide – 1/1000 dilution) for 30 minutes in dark. The cells were

treated with DAPI for nuclear staining. EdU- and DAPI-positive cells were quantified using MetaXpress cellular image analysis software (Molecular Devices).

SLC30A1 gene knockdown assay using small interfering RNA (siRNA)

Cells were seeded at 2000 cells/well in AKM (INS) medium. After 24 hours, cells were transfected with ON-TARGETplus Human SLC30A1 siRNA or ON-TARGETplus Non-targeting Control siRNA (Horizon Discovery) in DharmaFECT 1 transfection reagent (Horizon Discovery), following the manufacturer's protocol. Cell transfection was carried out in Opti-MEM Reduced Serum medium diluted with AKM (INS) medium for 24 hours. Transfected cells were treated with Compl and ΔMet media for 5 hours and were collected for RNA extraction or western blotting assay.

RNA sequencing

Ff-I01s01 undifferentiated hiPSCs were dissociated and plated at 5×10^5 cells/well on SynthemaxII-coated 6-well plates (Corning) and cultured at 37 °C for 24 hours. The cells were then treated with undifferentiated AKM (IGF1) medium with Zn addition (0, 0.5, 3, and 10 μM) described above and cultured for 48 hours. The cells were then dissociated and harvested. RNA was extracted using the RNeasy micro-kit (Qiagen, Germany) and DNase I (Qiagen) treatment was performed according to the manufacturer's instructions.

Library preparation and RNA sequencing were performed by Novagene Co. Ltd. Briefly, a total amount of 1 μg RNA per sample was used. Sequencing libraries were generated using NEBNext® UltraTM RNA Library Prep Kit for Illumina® (NEB, USA) following the manufacturer's instructions, and index codes were added to attribute sequences to each sample. The clustering of the index-coded samples was performed on a cBot Cluster Generation System using PE Cluster Kit cBot-HS (Illumina) according to the manufacturer's instructions. After cluster generation, the library preparations were sequenced on an Illumina platform (Novaseq 6000PE150) and paired-end reads were generated. Differential gene expression analysis was performed using the Subio platform (Subio).

Western blotting

Total protein extraction was performed with lysis buffer (10 mM Tris/HCl pH7.5, 0.5 mM $MgCl_2$ and 0.1% Triton X-100; recipe provided by Prof. Taiho Kambe, Kyoto University).

Proteins were separated in 8% SDS-PAGE with Mini-PROTEAN Electrophoresis System (Bio0Rad) and transferred to a PVDF (Millipore) membrane by Trans-Blot Semi-Dry Transfer Cell (Bio-Rad). Membranes were then blocked with 5% skimmed-milk (Morinaga Milk) in PBS-T and later incubate with primary antibodies. The primary antibodies were diluted with 5% skimmed-milk in PBS-T and incubated overnight at 4°C. Membranes were washed with PBS-T and incubated with HRP-linked secondary antibody for 2 hours at room temperature. Chemiluminescence band detection was performed by Immobilon Forte Western HRP Substrate (Millipore). Fusion solo S (Vilber Lourmat, France) was used for protein band visualization. Image J was used for quantification of the protein bands. The details of primary and secondary antibodies used are shown below.

Primary & Secondary Antibodies	Source	Product Code	Dilution
Mouse anti-ZNTI	Gifted by Prof. Taiho Kambe, Kyoto University	-	1:3000
β-Actin (D6A8) Rabbit mAb (HRP Conjugate)	Cell Signalling Technology, Inc.	12620	1:1000
HRP conjugated Goat-anti-mouse IgG	Jackson ImmunoResearch Inc.	115-035-146	1:3000

Measurement of metabolites in methionine cycle

Undifferentiated hiPSCs were replated at 5 $\times 10^5$ cells/well into 6-well-plate and cultured for 2-3 days in undiff-AKM (IGF1) with Zn addition (0 and 3 μM) media. The media were collected, and cells were harvested for metabolite analysis. Metabolites measurements were performed using ultra-high-performance liquid chromatography equipped with tandem mass spectrometry, TQD (UPLC-MS/MS; Waters) based on a previous report (Jiang et al., 2009). Separation was achieved using a PALL 10K omega column. Briefly, cells were lysed using three cycles of freeze/thaw in 50% methanol. Samples were deproteinized using 33% acetonitrile and evaporated completely. Each sample was injected, and concentrations were calculated based on the standard curve obtained from serial dilution of standard solution for each metabolite. Intracellular metabolites ($[Metabolite]_i$) are obtained by normalizing the metabolites to total protein (μmol / g total protein). Extracellular metabolites ($[Metabolite]_e$) are obtained by

subtracting the metabolites with reference (initially contained metabolites in the fresh medium) and normalized to 24 hours, and the cell number (nmol / 24h /1x10^6 cells).

Statistical Analysis

Data are expressed as mean ± SD (standard deviation). For comparisons of discrete data sets, two-tailed unpaired Student's *t*-tests, one-way ANOVA and Dunnett's multiple comparisons test were performed. Significant differences are indicated as **p*<0.05, ***p*<0.01 and ****p*<0.005 for Student's *t*-tests, $^{\S}p < 0.05$, $^{\S\S}p < 0.01$, $^{\S\S\S}p < 0.001$, $^{\S\S\S\S}p < 0.0001$ for one-way ANOVA and Dunnett's multiple comparisons test. All respective statistical analysis and p-value are noted in each figure legend..

References

Arakawa, A., Shiraki, N., Tsuyama, T., Kume, S., Iwahata, D., and Yamada, N. (2016). Speciation of Intracellular Zn, Fe and Cu within both iPS Cells and Differentiated Cells Using HPLC Coupled to ICP-MS. J. Anal. Bioanal. Tech. *7*, 1–8.

Baltaci, A.K., and Yuce, K. (2018). Zinc Transporter Proteins. Neurochem. Res. *43*, 517–530.

Barbato, J.C., Catanescu, O., Murray, K., DiBello, P.M., and Jacobsen, D.W. (2007). Targeting of metallothionein by L-homocysteine: a novel mechanism for disruption of zinc and redox homeostasis. Arterioscler. Thromb. Vasc. Biol. *27*, 49–54.

Becker, R.H.A., and Frick, A.D. (2008). Clinical pharmacokinetics and pharmacodynamics of insulin glulisine. Clin. Pharmacokinet. *47*, 7–20.

Cetin, I., Nobile De Santis, M.S., Taricco, E., Radaelli, T., Teng, C., Ronzoni, S., Spada, E., Milani, S., and Pardi, G. (2005). Maternal and fetal amino acid concentrations in normal pregnancies and in pregnancies with gestational diabetes mellitus. Am. J. Obstet. Gynecol. *192*, 610–617.

Chasapis, C.T., Spiliopoulou, C.A., Loutsidou, A.C., and Stefanidou, M.E. (2012). Zinc and human health: An update. Arch. Toxicol. *86*, 521–534.

Chen, G., and Wang, J. (2014). Threonine metabolism and embryonic stem cell self-renewal. Curr. Opin. Clin. Nutr. Metab. Care *17*, 80–85.

Chen, L., and Khillan, J.S. (2010). A novel signaling by vitamin A/retinol promotes self renewal of mouse embryonic stem cells by activating PI3K/Akt signaling pathway via insulin-like growth factor-1 receptor. Stem Cells *28*, 57–63.

Chimienti, F., Favier, A., and Seve, M. (2005). ZnT-8, a pancreatic beta-cell-specific zinc transporter. BioMetals *18*, 313–317.

Comes, S., Gagliardi, M., Laprano, N., Fico, A., Cimmino, A., Palamidessi, A., De Cesare, D., De Falco, S., Angelini, C., Scita, G., et al. (2013). L-proline induces a mesenchymal-like invasive program in embryonic stem cells by remodeling H3K9 and H3K36 methylation. Stem Cell Reports *1*, 307–321.

Danchin, A. (2020). Zinc, an unexpected integrator of metabolism? Microb. Biotechnol. *13*, 895–898.

Evans, J.C., Huddler, D.P., Jiracek, J., Castro, C., Millian, N.S., Garrow, T.A., and Ludwig, M.L. (2002). Betaine-Homocysteine Methyltransferase. Structure *10*, 1159–1171.

Fukada, T., and Kambe, T. (2011). Molecular and genetic features of zinc transporters in physiology and pathogenesis. Metallomics *3*, 662–674.

Furukawa, Y., Lim, C., Tosha, T., Yoshida, K., Hagai, T., Akiyama, S., Watanabe, S., Nakagome, K., and Shiro, Y. (2018). Identification of a novel zinc-binding protein, C1orf123, as an interactor with a heavy metalassociated domain. PLoS One *13*, 1–18.

Garg, S.K., Ellis, S.L., and Ulrich, H. (2005). Insulin glulisine: A new rapid-acting insulin analogue for the treatment of diabetes. Expert Opin. Pharmacother. *6*, 643–651.

González, B., Pajares, M.A., Martinez-Ripoll, M., Blundell, T.L., and Sanz-Aparicio, J. (2004). Crystal structure of rat liver betaine homocysteine S-methyltransferase reveals new oligomerization features and conformational changes upon substrate binding. J. Mol. Biol. *338*, 771–782.

Hu, J., Yang, Z., Wang, J., Yu, J., Guo, J., Liu, S., Qian, C., Song, L., Wu, Y., and Cheng, J. (2016). Zinc Chloride Transiently Maintains Mouse Embryonic Stem Cell Pluripotency by Activating Stat3 Signaling. PLoS One *11*, e0148994.

Huang, L. (2014). Zinc and its transporters, pancreatic β-cells, and insulin metabolism (Elsevier Inc.).

Huang, L., and Tepaamorndech, S. (2013). The SLC30 family of zinc transporters-A review of current understanding of their biological and pathophysiological roles. Mol. Aspects Med. *34*, 548–560.

Inoue, H., Nagata, N., Kurokawa, H., and Yamanaka, S. (2014). iPS cells: a game changer for future medicine. EMBO J. *33*, 409–417.

Jabrani, A., Makamte, S., Moreau, E., Gharbi, Y., Plessis, A., Bruzzone, L., Sanial, M., and Biou, V. (2017). Biophysical characterisation of the novel zinc binding property in Suppressor of Fused. Sci. Rep. *7*, 2–11.

Jeong, J., and Eide, D.J. (2013). The SLC39 family of zinc transporters. Mol. Aspects Med. *34*, 612–619.

Jiang, Z., Liang, Q., Luo, G., Hu, P., Li, P., and Wang, Y. (2009). HPLC-electrospray tandem mass spectrometry for simultaneous quantitation of eight plasma aminothiols: Application to studies of diabetic nephropathy. Talanta *77*, 1279–1284.

Kambe, T. (2019). Metalation and maturation of zinc ectoenzymes: A perspective. Biochemistry acs.biochem.9b00924.

Kambe, T., Tsuji, T., Hashimoto, A., and Itsumura, N. (2015). The physiological, biochemical, and molecular roles of zinc transporters in zinc homeostasis and metabolism. Physiol. Rev. *95*, 749–784.

Kimura, T., and Kambe, T. (2016). The functions of metallothionein and ZIP and ZnT transporters: An overview and perspective. Int. J. Mol. Sci. *17*, 10–12.

Koutmos, M., Pejchal, R., Bomer, T.M., Matthews, R.G., Smith, J.L., and Ludwig, M.L. (2008). Metal active site elasticity linked to activation of homocysteine in methionine synthases. Proc. Natl. Acad. Sci. U. S. A. *105*, 3286–3291.

Kroon, E., Martinson, L. a, Kadoya, K., Bang, A.G., Kelly, O.G., Eliazer, S., Young, H., Richardson, M., Smart, N.G., Cunningham, J., et al. (2008). Pancreatic endoderm derived from human embryonic stem cells generates glucose-responsive insulin-secreting cells in vivo. Nat. Biotechnol. *26*, 443–452.

Lemaire, K., Chimienti, F., and Schuit, F. (2012). Zinc transporters and their role in the pancreatic β-cell. J. Diabetes Investig. *3*, 202–211.

Liu, J., Qin, X., Pan, D., Zhang, B., and Jin, F. (2019). Amino Acid-Mediated Metabolism: A New Power to Influence Properties of Stem Cells. Stem Cells Int. *2019*.

Maret, W. (2000). The Function of Zinc Metallothionein: A Link between Cellular Zinc and Redox State. Am. Socirty Nutr. Sci. *130*, 1455–1458.

Matsuura, K., Kodama, F., Sugiyama, K., Shimizu, T., Hagiwara, N., and Okano, T. (2015). Elimination of remaining undifferentiated induced pluripotent stem cells in the process of human cardiac cell sheet fabrication using a methionine-free culture condition. Tissue Eng. - Part C Methods *21*, 330–338.

Millman, J.R., Xie, C., Van Dervort, A., Gürtler, M., Pagliuca, F.W., and Melton, D.A. (2016). Generation of stem cell-derived β-cells from patients with type 1 diabetes. Nat. Commun. *7*, 11463.

Mnatsakanyan, H., Serra, R.S.I., Salmeron-Sanchez, M., and Rico, P. (2019). Zinc maintains embryonic stem cell pluripotency and multilineage differentiation potential via AKT activation. Front. Cell Dev. Biol. *7*, 1–17.

Nishito, Y., and Kambe, T. (2019). Zinc transporter 1 (ZNT1) expression on the cell surface is elaborately controlled by cellular zinc levels. J. Biol. Chem. *294*, 15686–15697.

Pagliuca, F.W., Millman, J.R., Gürtler, M., Segel, M., Van Dervort, A., Ryu, J.H., Peterson, Q.P., Greiner, D., and Melton, D.A. (2014). Generation of Functional Human Pancreatic β Cells

In Vitro. Cell *159*, 428–439.

Pfaender, S., Föhr, K., Lutz, A.K., Putz, S., Achberger, K., Linta, L., Liebau, S., Boeckers, T.M., and Grabrucker, A.M. (2016). Cellular Zinc Homeostasis Contributes to Neuronal Differentiation in Human Induced Pluripotent Stem Cells. Neural Plast. *2016*.

Pound, L.D., Sarkar, S.A., Benninger, R.K.P., Wang, Y., Suwanichkul, A., Shadoan, M.K., Printz, R.L., Oeser, J.K., Lee, C.E., Piston, D.W., et al. (2009). Deletion of the mouse Slc30a8 gene encoding zinc transporter-8 results in impaired insulin secretion. Biochem. J. *421*, 371–376.

Rezania, A., Bruin, J.E., Arora, P., Rubin, A., Batushansky, I., Asadi, A., O'Dwyer, S., Quiskamp, N., Mojibian, M., Albrecht, T., et al. (2014). Reversal of diabetes with insulin-producing cells derived in vitro from human pluripotent stem cells. Nat. Biotechnol.

Roohani, N., Hurrell, R., Kelishadi, R., and Schulin, R. (2013). Zinc and its importance for human health: An integrative review. J. Res. Med. Sci. *18*, 144–157.

Rutter, G. a., and Chimienti, F. (2015). SLC30A8 mutations in type 2 diabetes. Diabetologia *58*, 31–36.

Ryu, J.M., and Han, H.J. (2011). L-threonine regulates G1/S phase transition of mouse embryonic stem cells via PI3K/Akt, MAPKs, and mTORC pathways. J. Biol. Chem. *286*, 23667–23678.

Saito, Y., Iwatsuki, K., Hanyu, H., Maruyama, N., Aihara, E., Tadaishi, M., Shimizu, M., and Kobayashi-Hattori, K. (2017). Effect of essential amino acids on enteroids: Methionine deprivation suppresses proliferation and affects differentiation in enteroid stem cells. Biochem. Biophys. Res. Commun. *488*, 171–176.

Sánchez Alvarado, A., and Yamanaka, S. (2014). Rethinking differentiation: Stem cells, regeneration, and plasticity. Cell *157*, 110–119.

Shahjalal, H.M., Shiraki, N., Sakano, D., Kikawa, K., Ogaki, S., Baba, H., Kume, K., and Kume, S. (2014). Generation of insulin-producing beta-like cells from human iPS cells in a defined and completely xeno-free culture system. J. Mol. Cell Biol. *6*, 394–408.

Shiraki, N., Shiraki, Y., Tsuyama, T., Obata, F., Miura, M., Nagae, G., Aburatani, H., Kume, K., Endo, F., and Kume, S. (2014). Methionine metabolism regulates maintenance and differentiation of human pluripotent stem cells. Cell Metab. *19*, 780–794.

Shyh-Chang, N., Locasale, J.W., Lyssiotis, C. a, Zheng, Y., Teo, R.Y., Ratanasirintrawoot, S., Zhang, J., Onder, T., Unternaehrer, J.J., Zhu, H., et al. (2013). Influence of threonine

metabolism on S-adenosylmethionine and histone methylation. Science *339*, 222–226.

Sim, E.Z., Shiraki, N., and Kume, S. (2021). Recent progress in pancreatic islet cell therapy. Inflamm. Regen. *41*, 1.

Suemori, H., Yasuchika, K., Hasegawa, K., Fujioka, T., Tsuneyoshi, N., and Nakatsuji, N. (2006). Efficient establishment of human embryonic stem cell lines and long-term maintenance with stable karyotype by enzymatic bulk passage. Biochem. Biophys. Res. Commun. *345*, 926–932.

Takahashi, S. (2012). Molecular functions of metallothionein and its role in hematological malignancies. J. Hematol. Oncol. *5*, 1–8.

Takahashi, K., and Yamanaka, S. (2006). Induction of Pluripotent Stem Cells from Mouse Embryonic and Adult Fibroblast Cultures by Defined Factors. Cell *126*, 663–676.

Takahashi, K., and Yamanaka, S. (2016). A decade of transcription factor-mediated reprogramming to pluripotency. Nat. Rev. Mol. Cell Biol. *17*, 183–193.

Takeda, T. aki, Miyazaki, S., Kobayashi, M., Nishino, K., Goto, T., Matsunaga, M., Ooi, M., Shirakawa, H., Tani, F., Kawamura, T., et al. (2018). Zinc deficiency causes delayed ATP clearance and adenosine generation in rats and cell culture models. Commun. Biol. *1*, 1–13.

Thirumoorthy, N., Kumar, K.T.M., Sundar, A.S., Panayappan, L., and Chatterjee, M. (2007). Metallothionein : An overview. World J. Gastroenterol. *13*, 993–996.

Thomson, J.A., Itskovitz-eldor, J., Shapiro, S.S., Waknitz, M.A., Swiergiel, J.J., Marshall, V.S., and Jones, J.M. (1998). Embryonic Stem Cell Lines Derived from Human Blastocysts. Science (80-.). *282*, 1145–1147.

Ueki, K., Okada, T., Hu, J., Chong, W.L., Assmann, A., Dahlgren, G.M., Peters, J.L., Shackman, J.G., Zhang, M., Artner, I., et al. (2006). Total insulin and IGF-I resistance in pancreatic β cells causes overt diabetes. Nat. Genet. *38*, 583–588.

Velazco-Cruz, L., Song, J., Maxwell, K.G., Goedegebuure, M.M., Augsornworawat, P., Hogrebe, N.J., and Millman, J.R. (2019). Acquisition of Dynamic Function in Human Stem Cell-Derived β Cells. Stem Cell Reports *12*, 351–365.

Wang, W.C., Mao, H., Ma, D.D., and Yang, W.X. (2014). Characteristics, functions, and applications of metallothionein in aquatic vertebrates. Front. Mar. Sci. *1*, 1–12.

Washington, J.M., Rathjen, J., Felquer, F., Lonic, A., Bettess, M.D., Hamra, N., Semendric, L., Tan, B.S.N., Lake, J.A., Keough, R.A., et al. (2010). L-proline induces differentiation of ES

cells: A novel role for an amino acid in the regulation of pluripotent cells in culture. Am. J. Physiol. - Cell Physiol. *298*, 982–992.

Werner, H., Weinstein, D., and Bentov, I. (2008). Similarities and differences between insulin and IGF-I: Structures, receptors, and signalling pathways. Arch. Physiol. Biochem. *114*, 17–22.

Wu, G., Bazer, F.W., Datta, S., Johnson, G.A., Li, P., Satterfield, M.C., and Spencer, T.E. (2008). Proline metabolism in the conceptus: Implications for fetal growth and development. Amino Acids *35*, 691–702.

Yanagisawa, H., and Nodera, M. (2007). Zinc Physiology and Clinical Practice. Biomed Res Trace Elem. *18 (1)*, 3–9.

Yang, M., Bao, D., Shi, A., Yuan, H., Wang, J., He, W., Tong, X., and Qin, H. (2020). Zinc Promotes Patient-Derived Induced Pluripotent Stem Cell Neural Differentiation via ERK-STAT Signaling. Stem Cells Dev. *29*, 863–875.

Yoshioka, N., Gros, E., Li, H., Kumar, S., Deacon, D.C., Maron, C., Muotri, A.R., Chi, N.C., Fu, X., Yu, B.D., et al. (2013). Efficient generation of human iPSCs by a synthetic self-replicative RNA. Stem Cell *13*, 246–254.

Zhang, D., Jiang, W., Liu, M., Sui, X., Yin, X., Chen, S., Shi, Y., and Deng, H. (2009). Highly efficient differentiation of human ES cells and iPS cells into mature pancreatic insulin-producing cells. Cell Res. *19*, 429–438.

Zoroddu, M.A., Aaseth, J., Crisponi, G., Medici, S., Peana, M., and Nurchi, V.M. (2019). The essential metals for humans: a brief overview. J. Inorg. Biochem. *195*, 120–129.

Achievements

- **Publications**

1. Erinn Zixuan Sim, Takayuki Enomoto, Nobuaki Shiraki, Nao Furuta, Soshiro Kashio, Taiho Kambe, Tomonori Tsuyama, Akihiro Arakawa, Hiroki Ozawa, Mizuho Yokoyama, Masayuki Miura and Shoen Kume. Methionine metabolism regulates pluripotent stem cell pluripotency and differentiation through zinc mobilization. *Cell Reports* **40**, 111120. (2022) https://doi.org/10.1016/j.celrep.2022.111120
2. Erinn Zixuan Sim, Nobuaki Shiraki and Shoen Kume. Recent progress in pancreatic islet cell therapy. *Inflammation and Regeneration* **41**, 1. (2021) https://doi.org/10.1186/s41232-020-00152-5

- **International Conference**

(Oral Presentation)

1. Zixuan Erinn Sim*, Saeko Momma, Nobuaki Shiraki, Shoen Kume

Title: A novel 3D spheroid culture system for generating functional pancreatic β cells derived from human induced pluripotent stem cells

Conference Name: Annual Meeting of the Japanese Society of Developmental Biologists

Venue: Tower Hall Funabori, Tokyo JAPAN

Date: 14th - 17th May 2017

Poster Number: OP01-05

(Poster Presentation)

1. Zixuan Erinn Sim*, Nobuaki Shiraki and Shoen Kume

Title: Insulin supplement is essential in differentiating human induced pluripotent stem cells into pancreatic beta cells

Conference Name: ISSCR 2019 Annual Meeting. Poster Number

Venue: LA Convention Center, Los Angeles USA

Date: 26th – 29th June 2019

Poster Number: F-3155

2. Zixuan Erinn Sim*, Nobuaki Shiraki and Shoen Kume

Title: Insulin supplement is essential in differentiating human induced pluripotent stem cells into pancreatic beta cells

Conference Name: 16th Asia-Oceania Congress of Endocrinology (AOCE) 2018

Venue: Royal Ambarrukmo Hotel, Yogyakarta INDONESIA

Date: 28th – 30th September 2018

(This poster presentation was being awarded as 'The 1st Winner of Free Paper Poster Presentation Award' during the conference.)

3. Zixuan Erinn Sim*, Saeko Momma, Nobuaki Shiraki, Shoen Kume

Title: A novel 3D spheroid culture system for generating functional pancreatic β cells derived from human induced pluripotent stem cells

Conference Name: ISSCR 2017 Annual Meeting

Venue: Boston Convention and Exhibition Center, Boston USA

Date: 14th – 17th June 2017

Poster Number: F-2044

4. Zixuan Erinn Sim*, Saeko Momma, Nobuaki Shiraki, Shoen Kume

Title: A novel 3D spheroid culture system for generating functional pancreatic β cells derived from human induced pluripotent stem cells

Conference Name: Annual Meeting of the Japanese Society of Developmental Biologists

Venue: Tower Hall Funabori, Tokyo JAPAN

Date: 14th – 17th May 2017

Poster Number: P024